Available online at www.sciencedirect.com
SCIENCE DIRECT®
Biochemical and Biophysical Research Communications 319 (2004) 103–113
BBRC
www.elsevier.com/locate/ybbrc

Sall1, a causative gene for Townes–Brocks syndrome, enhances the canonical Wnt signaling by localizing to heterochromatin

Akira Sato,[a,b] Shosei Kishida,[c] Toshiya Tanaka,[d] Akira Kikuchi,[c] Tatsuhiko Kodama,[d] Makoto Asashima,[b] and Ryuichi Nishinakamura[a,e,f,*]

[a] *Division of Stem Cell Regulation, The Institute of Medical Science, The University of Tokyo, Tokyo 108-8639, Japan*
[b] *Department of Life Sciences, The University of Tokyo, Tokyo 153-8902, Japan*
[c] *Department of Biochemistry, Faculty of Medicine, Hiroshima University 1-2-3, Kasumi, Minami-ku, Hiroshima 734-8551, Japan*
[d] *Laboratory for Systems Biology and Medicine, Research Center for Advanced Science and Technology, The University of Tokyo, Tokyo 153-8904, Japan*
[e] *Division of Integrative Cell Biology, Institute of Molecular Embryology and Genetics, Kumamoto University, Kumamoto 860-0811, Japan*
[f] *PREST, JST, Saitama 332-0012, Japan*

Received 12 April 2004

Abstract

The *Spalt* (*sal*) gene family plays an important role in regulating developmental processes of many organisms. Mutations of human *SALL1* cause the autosomal dominant disorder, Townes–Brocks syndrome (TBS), and result in ear, limb, anal, renal, and heart anomalies. Targeted deletion of mouse *Sall1* results in kidney agenesis or severe dysgenesis. Molecular mechanisms of *Sall1*, however, have remained largely unknown. Here we report that Sall1 synergistically activates canonical Wnt signaling. The transcriptional activity of Sall1 is related to its nuclear localization to punctate nuclear foci (pericentromeric heterochromatin), but not to its localization or association with β-catenin, the nuclear component of Wnt signaling. In contrast, the RNA interference of Sall1 reduces reporter activities of canonical Wnt signaling. The N-terminal truncated Sall1, produced by mutations often found in TBS, disturbs localization of native Sall1 to heterochromatin, and also down-regulates the synergistic transcriptional enhancement for Wnt signal by native Sall1. Thus, we propose a new mechanism for Wnt signaling activation, that is the heterochromatin localization of Sall1.

The *Spalt* (*sal*) gene family plays important roles in regulating developmental processes of many organisms. In *Drosophila* development, *sal* is a region-specific homeotic gene, which specifies cell fate decisions of chordontonal precursors in the peripheral nervous system [1,2], regulates tracheal development [3], controls terminal differentiation of photoreceptors [4], and determines proper placement of wing veins [5,6].

Humans have four *sal* related genes (*SALL1*, *SALL2*, *SALL3*, and *SALL4*) and mice also have four (*Sall1*, *Sall2*, *Sall3*, and *Sall4*) [7–15]. Heterozygous mutations of human *SALL1* lead to Townes–Brocks syndrome, with features of dysplastic ears, preaxial polydactyly, imperforate anus, and (less commonly) kidney and heart anomalies [16]. With homozygous deletion in mice the kidney had severe defects which meant that *Sall1* has an essential role in kidney development [17]. The molecular mechanisms of Sall1 have remained obscure.

Sall1 encodes a protein that contains 10 zinc finger motifs. The most N-terminal zinc finger is a single C2HCtype and is conserved only in vertebrates (*Drosophila sal* does not have the N-terminal C2HC zinc finger) [18]. The other zinc fingers are of the C2H2-type and are arranged as doublets with a third finger associated with the second pair. Recently, it was reported that Sall1 functions as a transcriptional repressor, by being localized to pericentromeric heterochromatin and is associated with histone deacetylase (HDAC) complex [19,20]. When linked to a heterologous DNA-binding

* Corresponding author. Fax: +81-96-373-6618.
E-mail address: ryuichi@kaiju.medic.kumamoto-u.ac.jp (R. Nishinakamura).

0006-291X/$ - see front matter © 2004 Elsevier Inc. All rights reserved.
doi:10.1016/j.bbrc.2004.04.156

domain (GAL4 DNA-binding domain), Sall1 protein is capable of repressing transcription on the synthetic reporter containing tandem GAL4-binding sites upstream of a promoter. The native DNA-binding site and direct target genes regulated by Sall1 proteins have remained to be determined.

In *Drosophila* wing development, *sal* is activated downstream of *dpp* (bone morphogenetic protein 4 ortholog) and in tracheal development is activated downstream of *wingless* (Wnt ortholog) [5,21–23]. We did research to determine if mammalian Sall1 is involved in signaling pathways related to development. We report here that Sall1 synergistically enhanced reporter activities of the canonical Wnt signal, by localizing to heterochromatin. Our evidence indicates that this mechanism may be related to the cause of TBS.

Materials and methods

Plasmids. The complete coding *Sall1* cDNA was fused to the HA-tag by replacing the PCR fragment amplified using the primer containing HA-tagged sequence and the *Sal*I restriction enzyme site (f, GTCGACA CCATGTACCCATACGACGTCCCAGACTACGCTTCGCGGAG GAAGCAAGCG; r, GAGCAGAAGGTCTGATAATTC). The *Sal*I–*Not*I digested HA-tagged *Sall1* cDNA fragment was cloned into the *Xho*I–*Not*I sites of pCAGEN, a mammalian expression vector driven by the CAG promoter [24,25].

Sall1 truncated forms were generated as follows; zinc finger region 1 (Zn 1) encoding 1–288 amino acids (*Sal*I-*Sac*I fragment) was inserted into pCAGEN vector, zinc finger region 2 (Zn 2) encoding 289–598 amino acids (*Sac*I–*Apa*I fragment), zinc finger region 3 (Zn 3) encoding 599–857 amino acids (*Apa*I–*Xho*I fragment), zinc finger region 4 (Zn 4) encoding 858–1105 amino acids (*Xho*I–*Spe*I fragment), and zinc finger region 5 (Zn 5) encoding 1106–1324 amino acids (*Spe*I–*Not*I fragment) were inserted into appropriate restriction sites in pCMV-HA vector (Clontech). The N-terminal half form of HA-tagged Sall1 encoding 1–598 amino acids (Zn1-2) was inserted into the pCAGEN vector, and the C-terminal half form encoding 599–1324 amino acids (Zn 3–5) inserted into the pCMV-HA vector.

The Sall1-GFP fusion was generated by inserting the d2EGFP fragment from pd2EGFP-1 vector (Clontech) at the 3′ terminal region of Sall1 in pBluescript II KS (−) vector in-frame. *Sal*I–*Not*I fragment of the Sall1-d2EGFP fusion was excised and inserted into the pCAGEN vector. To generate GFP-fused Sall1 truncated forms, the pCMV-HA-NLS-d2GFP vector was constructed. The PCR fragment coding a single nuclear localization signal from SV40 was inserted into the pCMV-HA vector (pCMV-HA-NLS vector) and then the fragment coding d2EGFP following intact multiple cloning sites excised from pd2EGFP-1 vector was inserted and the pCMV-HA-NLS-d2EGFP vector was generated. Sall1 truncated forms fused to d2EGFP were generated as follows; zinc finger region 1 encoding 1–288 amino acids (*Sal*I–*Sac*I fragment), zinc finger region 1–2 encoding 1–598 amino acids (*Sac*I–*Apa*I fragment), and zinc finger region 3–5 encoding 599–1324 amino acids (*Spe*I–*Not*I fragment) were inserted into appropriate restriction sites in pCMV-HA-NLS-d2EGFP vector (Clontech) in-frame. The cDNA fragment of zinc finger region 1′ (Zn 1′) encoding 1–435 amino acids was generated by the combination of the *Sal*I–*Sac*I fragment encoding 1–288 amino acids and the fragment encoding 299–435 amino acids that was amplified using primers containing *Sma*I restriction enzyme site in the reverse one (f, ATTAGC ACAGAGCCTTGCTAGC; r, CCCGGGGGACATTTGG TGGCTTGCTTTTTC). The combined cDNA fragment was inserted into the pCMV-HA-NLS-d2EGFP vector in-frame. The cDNA encoding zinc finger region 1′ (1–435 amino acids) without NLS was generated by combination of the *Sal*I–*Sac*I fragment encoding 1–288 amino acids and the fragment encoding 299–435 amino acids fused to d2EGFP, which was excised from the pCMV-HA-NLS-Zn 1′-d2EGFP vector, as described above, and inserted into appropriate sites in the pCAGEN vector. To generate the Zn 1′-DsRed2 fusion, the *Age*I–*Xho*I DsRed2 fragment without NLS was excised from pDsRed2-Nuc vector (Clontech), and inserted into the pCAGEN vector with the *Sal*I–*Age*I Zn 1′ fragment excised from the pCMV-HA-NLS-Zn 1′-d2EGFP vector.

The fragment coding the complete β-catenin cDNA was excised from pBJ-myc-β-catenin by *Bam*HI [26] and inserted into appropriate sites in the pCMV-myc vector (Clontech).

Protein interaction assay. BOSC23 cells were transiently transfected with 4 μg pCAGEN-HA-Sall1 or each pCMV-HA-Sall1 truncated form and 3 μg pCMV-myc-β-catenin. After 48 h, cells were washed with phosphate-buffered saline, lysed for 10 min on ice with 600 μl buffer A (10 mM Hepes–KOH, pH 7.8, 10 mM KCl, 1.5 mM $MgCl_2$, 0.05% NP-40, 0.5 mM DTT, and 10% v/v protease inhibitor cocktail for mammalian cell extract (SIGMA)), and spun at 2300*g* for 1 min. The supernatant was discarded and then the pellet was suspended in 300 μl buffer C (20 mM Hepes–KOH, pH 7.8, 500 mM NaCl, 1.5 mM $MgCl_2$, 0.5 mM DTT, and 10% v/v protease inhibitor cocktail for mammalian cell extract), rotated at 4 °C for 30 min and then spun at 20,000*g* for 30 min. The supernatant was diluted with an equal volume of buffer C containing 50% glycerol.

For the immunoprecipitation assay, the extract was diluted with an equal volume of buffer D (20 mM Hepes–KOH, pH 7.8, 1.5 mM $MgCl_2$, 0.5 mM DTT, and 10% v/v protease inhibitor cocktail for mammalian cell extract), twice the volume of the dilution buffer (25 mM Hepes–KOH, pH7.8, 2.5 mM EDTA, 0.1% NP-40, and 10% v/v protease inhibitor cocktail for mammalian cell extract) in a 1.5 ml micro tube and then incubated on ice for 10 min. After removal of particulate cell debris by centrifugation at 20,000*g* for 5 min, the supernatant was incubated overnight with 2 μg of anti-HA high affinity (Roche) at 4 °C. HA-tagged protein and its interacting proteins were isolated by precipitation with protein G–Sepharose beads (Amersham–Pharmacia) for 3 h at 4 °C. The beads were washed three times with wash buffer (20 mM Hepes–KOH, pH 7.8, 375 mM NaCl, 1 mM $ZnCl_2$, 1 mM EDTA, 0.5 mM DTT, 1% NP-40, 10% glycerol, and 1 mM PMSF) and eluted by boiling in Laemmli sample buffer. HA-tagged protein and its interacting proteins were separated by SDS–polyacrylamide gel electrophoresis on 8% gels, transferred to Immobilon Transfer Membranes (Millipore), blocked in 3% nonfat dried milk, and incubated with anti-HA antibody (Roche) or anti-myc antibody (SC-40, Santa Cruz Biotechnology). Antibody reactivity was detected using horseradish peroxidase-labeled secondary antibodies anti-mouse (KPL) and horseradish peroxidase-labeled secondary antibodies anti-rat (KPL) and ECL detection reagents (Amersham–Pharmacia).

Monoclonal antibody for human SALL1. To generate a monoclonal antibody for human SALL1, we cloned the cDNA fragment of human SALL1 encoding 258–499 amino acids amplified using primers containing *Kpn*I restriction site at the 5′ end (f, GGTACCCGCTTCT CAGAATGCAGACTTG; r, GGTACCTTGTGTTTGAAGAATGC CTC). The PCR fragment was cloned into the *Kpn*I sites of pBACsurf-1, which is a baculovirus transfer vector designed for expression of target proteins on the virion surface. Recombinant virus was produced, purified, and then immunized [27]. Monoclonal antibody for human SALL1 was obtained after screening by immunoblotting using the extract from HEK293 cells. These selected clones were cross-reactive for both human SALL1 and mouse Sall1 proteins.

Cell culture, transfection, and RNAi. NIH-3T3 cells and HEK293 cells were maintained in Dulbecco's modified Eagle's medium (SIGMA) containing 10% fetal bovine serum. For reporter assay, cells were plated in a 6-well plate at a density of 1×10^5 cells per well. For transfection of plasmids, FuGENE6 (Roche Molecular Biochemicals) was used according to the manufacturer's direction. For transfection

of double-stranded (ds) RNA oligos, LIPOFECTAMINE 2000 (Invitrogen) was used according to the manufacturer's direction. Five ds RNAi oligos for SALL1 were designed and synthesized by DHARMACON. Sequences of these oligos are as follows:

No. 6 (5′-AAGGUCUUUGGGAGUGACAGU-3′),
No. 7 (5′-AAGAGAAAUACCCUCAUAUCC-3′),
No. 15 (5′-AAUGAUUCAUCCUCAGUGGGU-3′),
No. 18 (5′-AAGGGUAAUUUGAAGCAGCAC-3′),
No. 21 (5′-AAGUUCCCAGAAAUGUUCCAG-3′).

The probe used for Northern blots was the *Kpn*I fragment of human SALL1 cDNA, excised from the pBACsurf-human SALL1 vector described above. For Western blotting, we used a monoclonal antibody for human SALL1 as described and a monoclonal antibody for GAPDH (Ambion).

Reporter assay. An internal control reporter pRLTKmini, which has the minimal thymidine kinase promoter, was constructed by removing the *Bgl*II–*Eco*RI fragment from the promoter region of pRLTK (Promega). TOPflash (Upstate Biotechnology) is a luciferase reporter containing three copies T cell factor (TCF) binding sites upstream of the thymidine kinase minimal promoter and FOPflash (Upstate Biotechnology) is the negative control for TOPflash containing mutant TCF binding sites. In the reporter assay using Wnt supernatant, 0.5 μg TOPflash or FOPflash reporter plasmid, 0.05 μg pRLTKmini control reporter plasmid were transiently introduced with 1.0 μg Sall1 or Sall1 truncated mutant expression plasmids in NIH3T3 cells. In the reporter assay using HEK293 cells, the same amounts of reporters were introduced with 0.1 μg pCAGEN-HA-Sall1. In the reporter assay using the N-terminal truncated Sall1 (Zn 1′) plasmid, 0.1–1.0 μg of this plasmid was transiently introduced with 0.1 μg pCAGEN-HA-Sall1 in HEK293 cells. After 24 h, the transfected cells were stimulated by threefold-diluted Wnt supernatants, produced from Wnt3a overexpressing L cells (ATCC) [28]. After 48 h, the transfected cells were lysed with 150 μl lysis buffer (50 mM Tris–HCl, pH 7.4, 150 mM NaCl, 1 mM EDTA, and 0.1% NP-40), frozen and thawed three times, and then spun at 20,000*g* for 10 min. The supernatant was then assayed using Dual-Luciferase Reporter Assay System (Promega). Luminescent reporter activity was measured using LUMAT LB 9507 luminometer (EG&G BERTHOLD). In the reporter assay using the β-catenin expression vector, 0.3 μg pCMV-myc-β-catenin with 0.1–1.0 μg pCAGEN-HA-Sall1 was transiently introduced into NIH3T3 cells. In HEK293 cells, 0.01 μg pCMV-myc-β-catenin with 0.01–0.1 μg pCAGEN-HA-Sall1 was used. Forty-eight hours after transfections, cells were used in the same way as described above. In the reporter assay combined with RNA interference, the final concentration 20 μM of each si RNA oligo was transfected in Opti-MEM (Invitrogen) as the serum free condition using LIPOFECTAMINE 2000 (Invitrogen). After 6 h, the serum free medium was replaced with Dulbecco's modified Eagle's medium (SIGMA) containing 10% fetal bovine serum, then reporter plasmids were transfected in the same way as described above. In all reporter assays, EGFP expression plasmid, pCMV-EGFP, was used to normalize the DNA content of the transfection. All transfections were normalized to *Renilla* luciferase activity and were replicated. All reporter assays were repeated at least three times and representative data are shown.

Analysis of protein localization by confocal microscopy and immunocytochemistry. Total 1.0 μg of Sall1-GFP fusion plasmid or Sall1 mutant GFP fusion plasmids or β-catenin plasmid was transiently introduced into NIH3T3 cells plated in Lab-Tek II Chamber Slide w/ Cover RS Glass Slide (Nalge Nunc International). Twenty-four hours after transfection, cells were fixed in phosphate-buffered saline (PBS) containing 2% paraformaldehyde, 0.1% Triton X-100, and 2 μg/ml of 4,6-diamidino-2-phenylindole (DAPI) at 4 °C for 20 min, washed for 5 min in PBS three times at room temperature, and then blocked with 10% goat serum at room temperature for 30 min. Cells were then incubated for 1 h at room temperature with an anti-myc antibody diluted in PBS containing 1% goat serum (1:1000), and detected using a rhodamine-conjugated secondary antibody anti-mouse (CHEMICON). The localization of proteins was detected using confocal microscopy Radiance 2100 (Bio-Rad).

Results

Sall1 has the potential to activate the canonical Wnt signaling

As the expression of *spalt* is regulated by several signaling pathways (*dpp*/BMP, *wingless*/Wnt, etc.) in *Drosophila* development, luciferase assays were done using several reporters to examine the potential involvement of mammalian Sall1. In following experiments, we selected and used two cell lines; NIH3T3 cells and HEK293 cells. Endogenous Sall1 was detected in HEK293 cells, in RNA and protein levels, but not in NIH3T3 cells (data not shown). Among reporters tested (BMP, TGF-β, retinoic acid, LIF, and Wnt) [25,29–32], the Wnt responsive reporter consistently showed a synergistic response to Sall1 (Figs. 1A and B) in both cell lines. Sall1 expression vector was introduced with the Wnt responsive reporter (TOPflash) that contains multiple TCF binding sites or the control reporter (FOPflash), and these cells were stimulated by the supernatant from L cells stably expressing Wnt-3A. Sall1 alone only weakly activated the TOPflash reporter in both cell lines. In the presence of Wnt stimulation, however, Sall1 synergistically activated the TOPflash reporter in both cell lines, but not so the control FOPflash reporter. Therefore, Sall1 synergistically activates the canonical Wnt signal. In these settings, activation status of β-catenin was not altered as determined by Western blotting, ruling out the possibility of a secondary production of Wnt ligands by Sall1 or Wnt stimulation upstream of β-catenin (data not shown).

When the canonical Wnt pathway is activated, β-catenin avoids the ubiquitin–proteosome pathway following the phosphorylation by GSK3-β and accumulates in the cytoplasm to move into the nucleus and function as the transcriptional coactivator of the TCF/LEF transcription factor [33]. In NIH3T3 cells, expression of β-catenin alone activated gene expression on the TOPflash reporter only slightly, but co-expression of Sall1 and β-catenin synergistically increased its reporter activity in dependent manner regarding the amount of Sall1 (Fig. 1C). In HEK293 cells, Sall1 also enhanced the luciferase reporter by β-catenin (Fig. 1D). Sall1 by itself could not bind to TCF binding sites in the TOPflash reporter, as determined by an electromobility shift assay using nuclear extracts from Sall1-introduced HEK293 cells (data not shown). Therefore, Sall1 may possibly function as a coactivator for β-catenin in the canonical Wnt signaling.

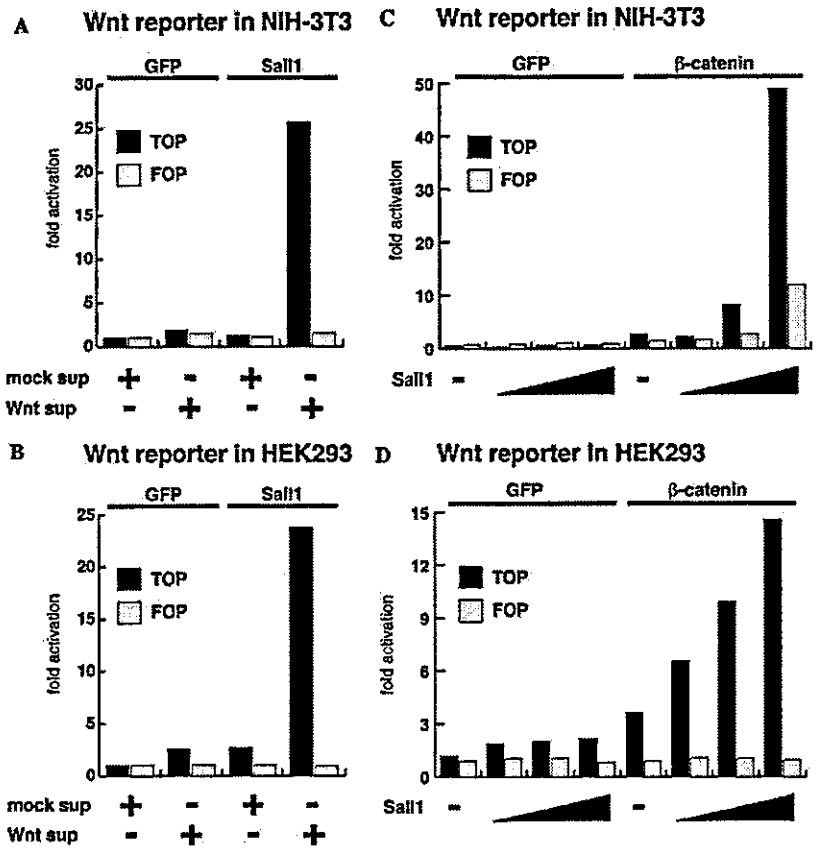

Fig. 1. Sall1 synergistically enhanced canonical Wnt signaling pathway. (A,B) The reporter assay responsive to Wnt signaling. TOPflash as the reporter plasmid responsive to Wnt signaling, FOPflash as negative control were introduced into NIH-3T3 cells (A), HEK293 cells (B). These cells were stimulated by the Wnt supernatant (Wnt sup) from L cell stably expressing Wnt-3A or the mock supernatant (mock sup) from normal L cells. (C,D) TOPflash reporter assay by expression of β-catenin, with or without Sall1. pCMV-myc-β-catenin (0.3 μg) (the β-catenin expression vector) and 0.1–1.0 μg of pCAGEN-HASall1 were introduced in NIH-3T3 cells (C). pCMV-myc-β-catenin (0.01 μg) (the β-catenin expression vector) and 0.01–0.1 μg of pCAGEN-HASall1 were introduced in HEK293 cells (D). In all reporter assays, pCMV-EGFP (the control vector) was used to normalize the DNA content of the transfection, and pRLTKmini was used as the internal control reporter plasmid.

Endogenous Sall1 participates in Wnt signaling in HEK293 cells

To determine if Sall1 endogenously participates in canonical Wnt signaling, we depleted the endogenous human SALL1 protein in HEK293 cells via double-strand RNA (siRNA)-mediated interference and did reporter assays. We designed five kinds of ds RNAi oligos for human SALL1 (Nos. 6, 7, 15, 18, and 21), and assessed their potential to deplete endogenous SALL1 mRNA, using Northern blot analysis (Fig. 2A). Oligo No. 18 most effectively, and Nos. 6 and 7 weakly, reduced endogenous SALL1 mRNA in HEK293 cells, but No. 21 had no effect (Fig. 2A). Therefore, we selected No. 21 as a negative control in following experiments, as it did not reduce the amount of either SALL1 or GAPDH (Figs. 2B and C). When used in reporter assays, oligo No. 18 most effectively, oligo No. 6 less effectively, down-regulated the activity on the TOPflash reporter, in proportion to their efficiency to reduce endogenous SALL1 mRNA, while a negative control, No. 21, did not do so (Fig. 2D). Therefore, endogenous SALL1 also participates in canonical Wnt signaling, at least in HEK293 cells.

Sall1 interacts with β-catenin

We next did immunoprecipitation studies to examine the interaction between Sall1 and β-catenin. Nuclear extracts were prepared from BOSC23 cells, transiently introduced with both HA-tagged Sall1 and myc-tagged β-catenin expression vectors. In these extracts, Sall1 effectively interacted with β-catenin (Fig. 3B). To further determine the domains of Sall1 required for interactions with β-catenin, we also did immunoprecipitation studies using deletion mutants of Sall1 with β-catenin. Sall1 has a total of 10 zinc fingers including multiple double-zinc finger motifs and we constructed five truncated mutants

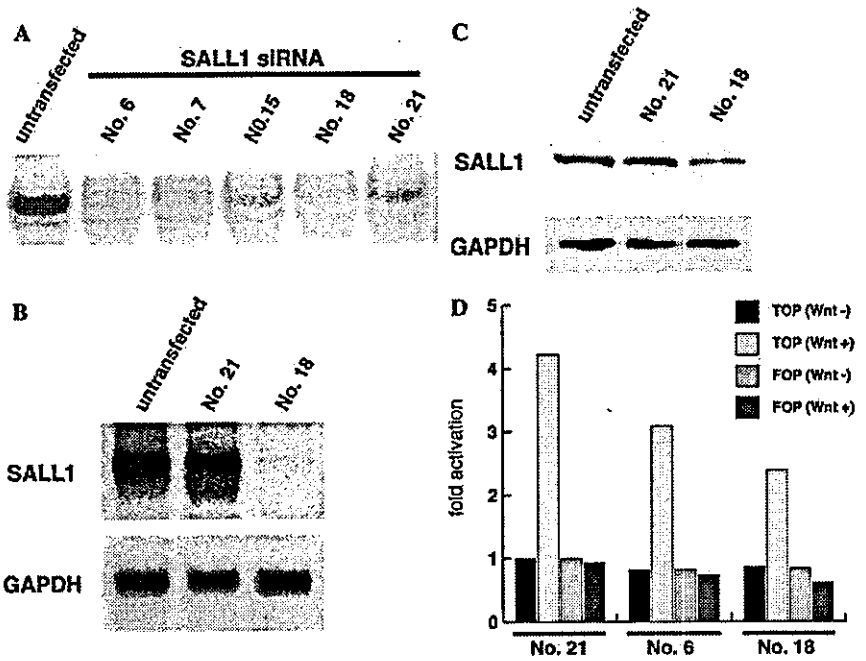

Fig. 2. RNA interference for endogenous Sall1 specifically down-regulates the TOPflash activity in HEK293 cells. (A,B) Northern analysis for assessing the efficiency of five designed siRNA oligos for human SALL1 to reduce the amount of endogenous SALL1 mRNA. (C) Western analysis for assessing the efficiency of SALL1 siRNA oligos to reduce the amount of endogenous SALL1 protein. (D) The reporter assay using SALL1 siRNA oligos in HEK293 cells. siRNA oligo, No. 18 most efficiently, and No. 6 less efficiently, down-regulated the reporter activity on TOPflash reporter in proportion to its efficiency to reduce endogenous SALL1 mRNA, while No. 21 had no effect.

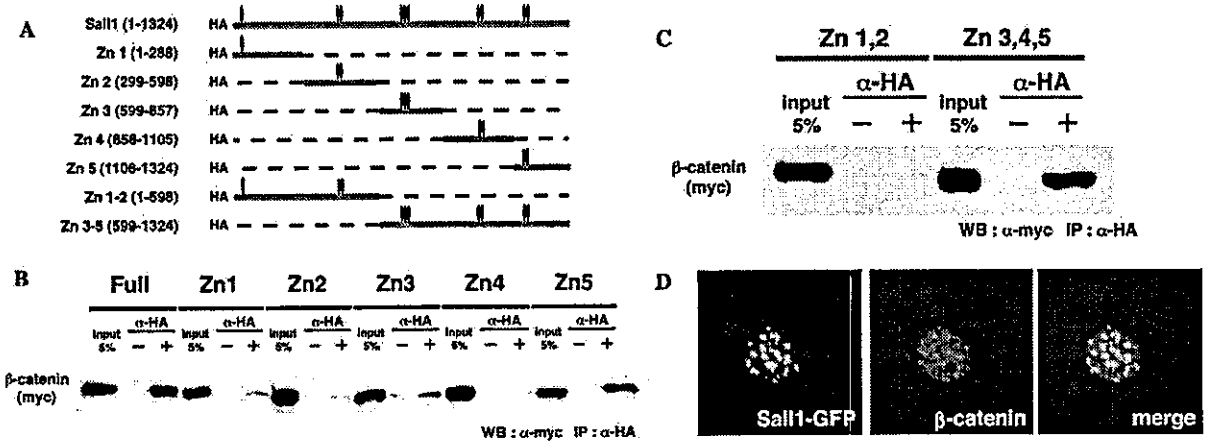

Fig. 3. Localization of Sall1, which has the potential to associate with β-catenin, does not overlap with those of β-catenin in the nucleus. (A) Diagram of HA-tagged full-length Sall1 and its deletion mutants used in protein interaction assays. Positions of the zinc fingers are depicted as ovals. The numbers in parentheses indicate the number of coding amino acids. (B,C) Protein interaction assay by immunoprecipitation using nuclear extracts from BOSC23 cells, transiently introduced with myc-β-catenin and HA-Sall1 or its mutants. Immunoprecipitation was done using an anti-HA antibody and detected using an anti-myc antibody. (D) The localization of Sall1 in the nucleus did not overlap with that of β-catenin. NIH3T3 cells on glass coverslips were transfected with full-length Sall1-GFP and myc-tagged β-catenin, stained with anti-myc. Cells were viewed using confocal microscopy.

encoding clusters of each zinc finger motif (Zn 1, 2, 3, 4, and 5) (Fig. 3A). The immunoprecipitation was done using lysates from BOSC23 cells introduced with these truncated mutants and β-catenin. The truncated form, encoding the most C-terminal double-zinc finger (Zn 5), had the highest affinity with β-catenin, and the form encoding the triple Zn finger (Zn 3) had a lesser affinity for β-catenin (Fig. 3B). To confirm these results, we

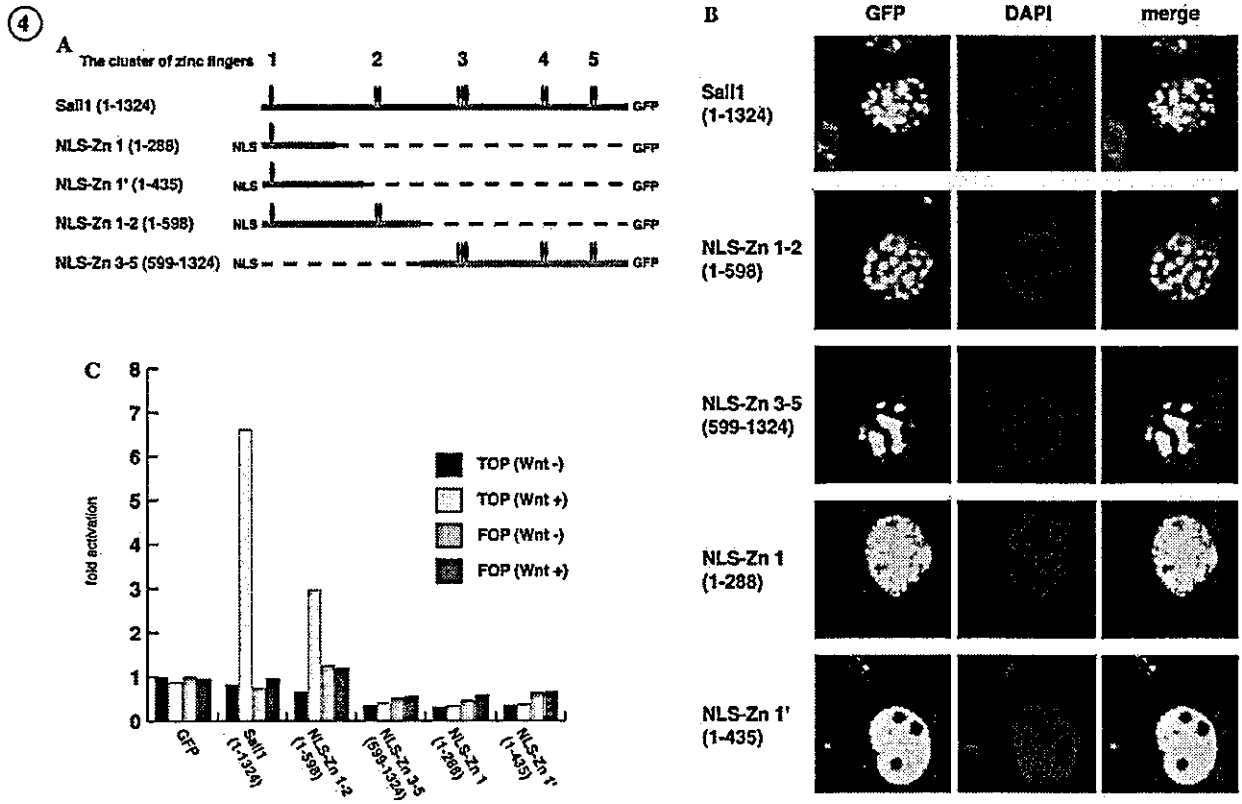
4
A
The cluster of zinc fingers 1 2 3 4 5
Sall1 (1-1324)
NLS-Zn 1 (1-288)
NLS-Zn 1' (1-435)
NLS-Zn 1-2 (1-598)
NLS-Zn 3-5 (599-1324)
NLS
GFP
B
GFP
DAPI
merge
Sall1 (1-1324)
NLS-Zn 1-2 (1-598)
NLS-Zn 3-5 (599-1324)
NLS-Zn 1 (1-288)
NLS-Zn 1' (1-435)
C
fold activation
TOP (Wnt -)
TOP (Wnt +)
FOP (Wnt -)
FOP (Wnt +)
GFP
Sall1 (1-1324)
NLS-Zn 1-2 (1-598)
NLS-Zn 3-5 (599-1324)
NLS-Zn 1 (1-288)
NLS-Zn 1' (1-435)

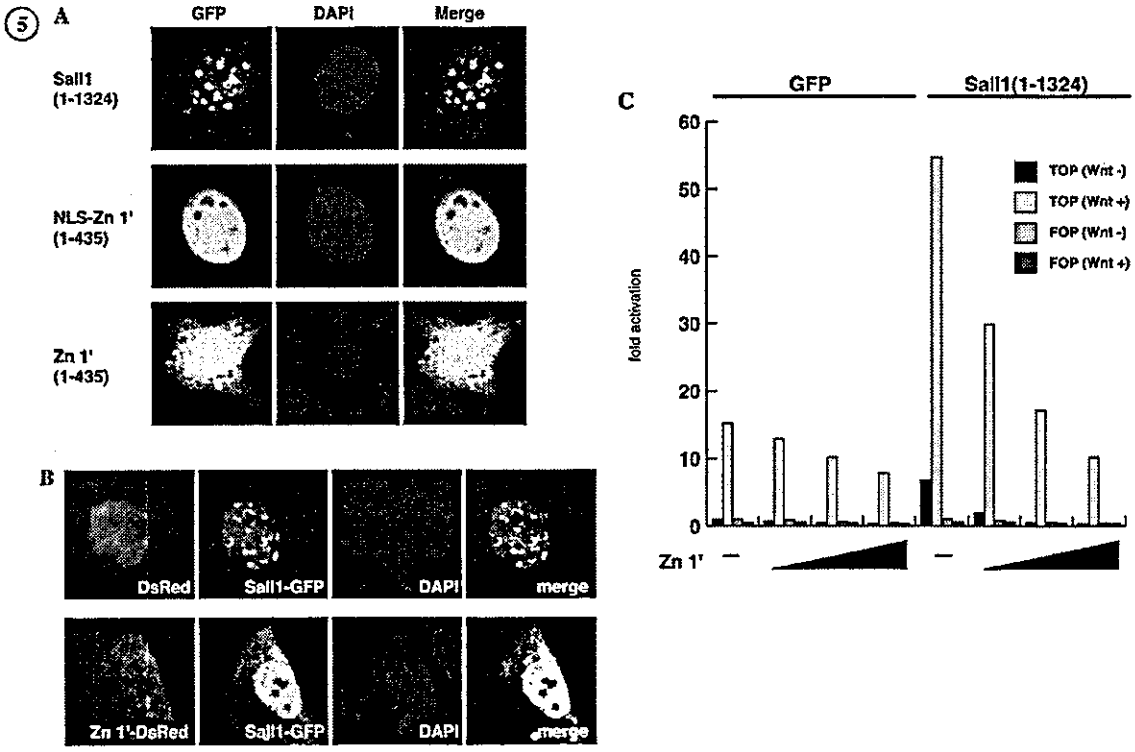
5
A
GFP
DAPI
Merge
Sall1 (1-1324)
NLS-Zn 1' (1-435)
Zn 1' (1-435)
B
DsRed
Sall1-GFP
DAPI
merge
Zn 1'-DsRed
Sall1-GFP
DAPI
merge
C
GFP
Sall1(1-1324)
fold activation
TOP (Wnt -)
TOP (Wnt +)
FOP (Wnt -)
FOP (Wnt +)
Zn 1'

divided Sall1 into halves and constructed two other mutant forms; Zn 1–2, the N-terminal half of Sall1, encoded first and second Zn finger regions, and Zn 3–5, the C-terminal half, encoded third, fourth, and fifth Zn finger regions (Fig. 3A). β-Catenin strongly interacted with the C-terminal half domain encoding Zn 3–5, but not with the N-terminal half domain encoding Zn 1–2 (Fig. 3C).

We next assessed whether the localization of Sall1 in the nucleus correlated with those of β-catenin in NIH3T3 cells, because NIH3T3 cells were useful to distinguish between euchromatic and heterochromatic regions than in HEK293 cells by confocal microscopy. Sall1 was localized to punctate nuclear foci (pericentromeric heterochromatin) as reported [19,20]. β-Catenin in the nucleus was also localized to the punctate nuclear foci, but its localization pattern only partially overlapped with Sall1 (Fig. 3D). This suggests that not all Sall1 in nucleus associates with β-catenin. We also assessed whether, upon Wnt stimulation, the localization pattern of Sall1 changes to overlap with that of β-catenin. Sall1 localization, however, did not change with or without Wnt stimulation (data not shown). Thus, Sall1 is not a simple coactivator for β-catenin on the TOPflash reporter.

The transcriptional activity of Sall1 correlates with its localization in the nucleus

Recently, Sall1 was reported to localize to punctate nuclear foci (pericentromeric heterochromatin) and its nuclear localization to correlate with its transcriptional repression [19,20]. We categorized 10 zinc fingers of Sall1 to five clusters of zinc fingers (Zn 1, 2, 3, 4, and 5) (Fig. 4A). To assess whether the localization of Sall1 in the nucleus also correlates with its transcriptional activation in Wnt signaling, we constructed Sall1-GFP or Sall1 mutants-GFP (Fig. 4A) and examined localization of these GFP-fusion proteins in NIH-3T3 cells using confocal microscopy (Fig. 4B). To focus localization of those mutants only in nucleus, the nuclear localization signal from SV40 was fused to the N-terminal of each GFP-fusion mutant. The full-length Sall1-GFP was localized as a small speckled pattern in the nucleus and co-localized with 4,6-diamidino-2-phenylindole (DAPI) and heterochromatin protein 1 (HP1), as reported [19,20] (Fig. 4B and data not shown). The N-terminal half of Sall1, Zn 1–2, was also localized in a similar fashion to the full-length Sall1, but localization of the C-terminal half, Zn 3–5, looked different; larger speckles or aggregates than those of the full-length and N-terminal half of Sall1-GFP (Fig. 4B). It was reported that the most N-terminal zinc finger domain that binds to HDAC complex is essential and sufficient for its repressor activity [19]. Therefore, we constructed Zn 1′ encoding 1–435 amino acids, which was reported to be the minimal truncated form as a transcriptional repressor (Fig. 4A). Unexpectedly, Zn 1′, which was reported to localize to heterochromatin in COS-1 cells, showed a uniform localization in the nucleus (Fig. 4B). The most N-terminal single zinc finger region, Zn 1, also showed uniform localization in the nucleus (Fig. 4B). Therefore, its localization to heterochromatin requires both the N-terminal single zinc finger (Zn 1) and the following double zinc fingers (Zn 2).

We next did luciferase reporter assays using full-length Sall1 protein and these Sall1 truncated forms. NIH-3T3 cells, introduced with these truncated Sall1 expression plasmids and TOPflash reporter, were stimulated by Wnt supernatants (Fig. 4C). Interestingly, Zn 3–5 (C-terminal half), that has the potential to bind β-catenin, had no activity in the luciferase assay. In contrast, Zn 1–2 (N-terminal half), that has the capacity to localize to heterochromatin, activated the TOPflash reporter, regardless of no interaction with β-catenin (Figs. 3B and C). This indicates Sall1 localization to heterochromatin, but not its association with β-catenin, correlates with its transcriptional activation in Wnt signaling. As Zn 1 and Zn 1′, which have only the first zinc finger, did not show synergistic enhancement of the reporter activity nor localization to heterochromatin, both zinc finger regions 1 and 2 are required for localization to heterochromatin and its synergistic transcriptional enhancement in Wnt signaling.

Fig. 4. The N-terminal half region of Sall1 has the potential to be localized to heterochromatin and to enhance synergistically Wnt reporter activity. (A) Diagram of GFP fused full-length Sall1 and its deletion mutants used in the confocal microscopy. Mutants are fused to NLS in N-terminus and to EGFP in C-terminus. (B) NIH3T3 cells grown on glass coverslips were transfected with corresponding deletion mutants of Sall1-GFP (green) or Sall1-truncated mutants-GFP, counterstained with DAPI (blue) to identify heterochromatin in nucleus, and viewed using confocal microscopy. (C) The reporter assay responsive to Wnt signaling using Sall1-GFP or Sall1 mutants-GFP plasmids. NIH3T3 cells were transfected with 1.0 μg of each Sall1-GFP or Sall1 mutants-GFP, and after 24 h, stimulated with Wnt sup or the mock sup.

Fig. 5. Zn 1′, which is produced by mutations often observed in human TBS, disrupts the localization of native Sall1 protein and its transcriptional activity in Wnt signaling in a dominant-negative fashion. (A) NIH3T3 cells were transfected with corresponding deletion mutants of Sall1-GFP (green), NLS-Zn 1′-GFP, or Zn 1′-GFP without NLS, and stained with DAPI (blue), and viewed using confocal microscope. (B) Full-length Sall1-GFP was introduced into NIH3T3 cells, together with DsRed (upper panels) or Zn 1′-DsRed (lower panels). DAPI staining (blue) shows heterochromatin. (C) The reporter assay responsive to Wnt signaling using the N-terminal truncated mutant Zn 1′. HEK293 cells were transfected with 0.1–1.0 μg Zn 1′ plasmid with or without 0.1 μg HA-Sall1 plasmid in addition to reporter plasmids, and after 24 h, stimulated by the Wnt sup or the mock sup.

Zn 1′, which is produced by mutations often observed in human TBS, disrupts the localization of native Sall1 protein and its transcriptional activity in Wnt signaling in a dominant-negative fashion

It was recently reported that mice carrying a mutation which caused the production of the truncated Sall1 protein, Zn 1′, recapitulated the abnormalities found in human TBS [34,35]. We confirmed that Zn 1′-GFP protein without NLS was localized uniformly in the cytoplasm and in the nucleus, as reported (Fig. 5A). As Zn 1′ was also reported to associate with all Sall family members, probably through the conserved N-terminal glutamine-rich domain [34,36], we hypothesized that Zn 1′ without NLS may affect the localization of native Sall1 protein and its synergistic enhancement of Wnt signaling. We constructed Zn 1′ protein fused to DsRed, introduced it with full-length Sall1-GFP fusion in NIH-3T3 cells, and examined the localization of these proteins using confocal microscopy. When co-expressed with the control DsRed protein, full-length Sall1-GFP remained to be localized to heterochromatin (Fig. 5B). Zn 1′ fused to DsRed, however, affected the localization of Sall1-GFP; Sall1-GFP was localized in both the cytoplasm and the nucleus. Sall1-GFP in the nucleus was no longer localized to heterochromatin, being uniformly localized together with Zn 1′-DsRed (Fig. 5B). This indicates that Zn 1′ functions as a dominant-negative form for native Sall1 proteins, by inhibiting the native Sall1 from localizing to heterochromatin. To assess whether Zn 1′ also functions as the dominant-negative form in Wnt signaling, we next did luciferase reporter assays of HEK293 cells using the Zn 1′ truncated forms without NLS. As HEK293 cells express endogenous Sall1, Zn 1′ introduction down-regulated the activity of endogenous Sall1 on the TOPflash reporter in a dose-dependent manner (Fig. 5C). When introduced with exogenous native Sall1, Zn 1′ also efficiently inhibited synergistic activation of the Wnt responsive reporter by native Sall1 (Fig. 5C). This indicates that the N-terminal truncated Sall1, Zn 1′, which is caused by high-frequent mutations in TBS, also functions as a dominant-negative form in canonical Wnt signaling. We propose that this newly defined mechanism of Wnt signaling activation by heterochromatin localization of Sall1 may explain one of the causative mechanisms of TBS.

Discussion

Sall plays important roles in a variety of organs, but its molecular mechanisms have remained largely unknown.

Here we show that Sall1 functions as a transcriptional activator specifically in the canonical Wnt signaling pathway. The luciferase activity on the TOPflash reporter stimulated by Wnt-3a was synergistically activated by the introduction of Sall1 (Fig. 1). We also tested other unrelated zinc finger proteins on the TOPflash reporter, and found that the effect on Wnt canonical pathway was specific to Sall1 (data not shown). The synergistic activity on TOPflash reporter by Sall1 was also observed by transfection of β-catenin and Sall1. The introduction of ds RNAi oligo for human SALL1 to HEK293 cells not only reduced the amount of endogenous SALL1 protein, but also led to down-regulation of the TOPflash reporter activity (Fig. 2). Activation of Wnt signaling by Sall1 did not correlate with its localization with β-catenin, but rather with its localization of heterochromatin (Figs. 3 and 4). Further, the N-terminal truncated form of Sall1 (Zn 1′), which was reported to lead human TBS abnormalities in mice [34], disturbed localization of the native Sall1 and also down-regulated the synergistic activity on TOPflash reporter by native Sall1 (Fig. 5).

In two previous reports, Sall1 was seen to function as a transcriptional repressor on the artificial promoter containing tandem GAL4 binding sites, when linked to the heterologous GAL4 DNA-binding domain, and also that Sall1 associated with HDAC and several components of the chromatin remodeling complex (MTA1, MTA2, and RbAp46/48) [20,34]. Therefore, Sall1 could repress gene expression by recruiting the HDAC complex. It was not, however, reported that native Sall1 functions as a transcriptional repressor. We found that the native form of Sall1 could function as a transcriptional activator in Wnt signaling essential for many developmental processes and that its activity correlated with its localization to heterochromatin [37]. The increase of Sall1 proteins may squelch some transcriptional repressor complex, including HDAC, or be associated with chromatin remodeling factors to alter the chromatin structure near the promoter region of Wnt target genes.

Another C2H2 type zinc finger protein Ikaros functions as both transcriptional repressor and activator, and is localized to pericentromeric heterochromatin [38–40]. Ikaros associates with DNA-dependent ATPase Mi-2 included in the NuRD chromatin remodeling complex [41]. Ikaros has six C2H2 type zinc fingers; the N-terminal zinc finger cluster consisting of four zinc fingers functions as the DNA-binding domain and C-terminal two zinc fingers as a dimerization domain [42]. When linked to a heterologous GAL4 DNA-binding domain, Ikaros functions as a transcriptional repressor on the reporter containing tandem GAL4 binding sites. On the other hand, the native form of Ikaros enhances activity of the reporter that contains tandem Ikaros binding sites upstream of the thymidine kinase promoter, and also enhances activity of the reporter containing no Ikaros binding sites but only Sp1

transcription factor binding sites. When Ikaros is not localized to heterochromatin caused by point mutations in its DNA-binding domain or dimerization domain, Ikaros does not enhance activities of these reporters. Therefore, localization of Ikaros to heterochromatin correlates with its transcriptional activation [38]. It was also reported that Sall proteins interact with all family members through its conserved glutamine-rich domain [36]. Therefore, a similar mechanism may function both for Sall1- and Ikaros-dependent activation. As the Zn 1–2 region of Sall1 was required and is sufficient for its heterochromatin localization (Fig. 4), these zinc fingers may bind to target sequences in heterochromatin, directly or indirectly. The identification of DNA sequences or molecules in heterochromatin compartments, which are required for heterochromatin localization of Sall1, would elucidate the mechanism of heterochromatin localization of Sall1 and eventually the mechanism of the activation of Wnt signaling by Sall1.

It is to be noted that Sall1-dependent activation is not general but rather it is specific to Wnt, at least among several pathways tested (BMP, TGF-β, retinoic acid, and LIF). The Wnt signal is regulated by multiple steps and large numbers of agonists and antagonists bind to β-catenin and TCF [26,43–48]. In addition, there is emerging evidence that more complicated mechanisms function in Wnt activation, including the transcriptional regulation by remodeling chromatin structure and by sumoylation [49,50]. In the former mechanism, it was reported that Brahma (Brm)/Brahma-related gene-1 (Brg-1), a component of mammalian SWI/SNF or RSC chromatin remodeling complex, binds to β-catenin, changes the chromatin structure by its ATPase activity, and then enhances Wnt-dependent transcription [49]. On the other hand, when an ARID domain protein Osa is contained in the Brm/Brg-chromatin remodeling complex, it tightens the chromatin structure and represses Wnt-dependent gene expression [50]. In the latter mechanism, the sumoylation of Lef-1 by PIASy, a member of E3 SUMO ligase, transfers Lef-1 to the nuclear body, a specific subcompartment in the nucleus, and then suppresses its transcriptional activity [51]. Tcf-4 is also sumoylated by PIASy, transferred to the PML nuclear body, and activates Wnt-dependent transcription [52]. It is to be noted that Sall1 also interacts with SUMO-1 and ubiquitin-conjugation enzyme UBE2I (human homolog of yeast UBC9), and is sumoylated [53], though its physiological relevance to Wnt signal remains to be determined. In this study, we propose another mechanism of Wnt signal activation by heterochromatin localization of Sall1. Further elucidation of this mechanism will lead to better understanding of not only the Wnt signal but also phenotypes observed in various species ranging from *Drosophila* to humans lacking SALL/spalt functions.

Acknowledgments

Akira Sato is supported by the Japan Society for the Promotion of Science. The Division of Stem Cell Regulation is supported by Amgen Limited.

References

[1] P.R. Elstob, V. Brodu, A.P. Gould, Spalt-dependent switching between two cell fates that are induced by the *Drosophila* EGF receptor, Development 128 (2001) 723–732.
[2] T.E. Rusten, R. Cantera, J. Urban, G. Technau, F.C. Kafatos, R. Barrio, Spalt modifies EGFR-mediated induction of chordontonal precursors in the embryonic PNS of *Drosophila* promoting the development of oenocytes, Development 128 (2001) 711–722.
[3] M. Boube, M. Llimargas, J. Casanova, Cross-regulatory interactions among tracheal genes support a co-operative model for the induction of tracheal fates in the *Drosophila* embryo, Mech. Dev. 91 (2000) 271–278.
[4] B. Mollereau, M. Dominguez, R. Webel, N.J. Colley, B. Keung, J.F. de Celis, C. Desplan, Two-step process for photoreceptor formation in *Drosophila*, Nature 412 (2001) 911–913.
[5] J.F. de Celis, R. Barrio, F.C. Kafatos, A gene complex acting downstream of dpp in *Drosophila* wing morphogenesis, Nature 381 (1996) 421–424.
[6] J.F. de Celis, R. Barrio, Function of the spalt/spalt-related gene complex in positioning the veins in the *Drosophila* wing, Mech. Dev. 91 (2000) 31–41.
[7] A. Buck, L. Archangelo, C. Dixkens, J. Kohlhase, Molecular cloning, chromosomal localization, and expression of the murine SALL1 ortholog Sall1, Cytogenet. Cell Genet. 89 (2000) 150–153.
[8] J. Kohlhase, M. Altmann, L. Archangelo, C. Dixkens, W. Engel, Genomic cloning, chromosomal mapping, and expression analysis of msal-2, Mamm. Genome 11 (2000) 64–68.
[9] J. Kohlhase, S. Hausmann, G. Stojmenovic, C. Dixkens, K. Bink, W. Schulz-Schaeffer, M. Altmann, W. Engel, SALL3, a new member of the human spalt-like gene family, maps to 18q23, Genomics 62 (1999) 216–222.
[10] J. Kohlhase, R. Schuh, G. Dowe, R.P. Kuhnlein, H. Jackle, B. Schroeder, W. Schulz-Schaeffer, H.A. Kretzschmar, A. Kohler, U. Muller, M. Raab-Vetter, E. Burkhardt, W. Engel, R. Stick, Isolation, characterization, and organ-specific expression of two novel human zinc finger genes related to the *Drosophila* gene spalt, Genomics 38 (1996) 291–298.
[11] T. Ott, K.H. Kaestner, A.P. Monaghan, G. Schutz, The mouse homolog of the region specific homeotic gene spalt of *Drosophila* is expressed in the developing nervous system and in mesoderm-derived structures, Mech. Dev. 56 (1996) 117–128.
[12] T. Ott, M. Parrish, K. Bond, A. Schwaeger-Nickolenko, A.P. Monaghan, A new member of the spalt like zinc finger protein family, Msal-3, is expressed in the CNS and sites of epithelial/mesenchymal interaction, Mech. Dev. 101 (2001) 203–207.
[13] J. Kohlhase, M. Heinrich, L. Schubert, M. Liebers, A. Kispert, F. Laccone, P. Turnpenny, R.M. Winter, W. Reardon, Okihiro syndrome is caused by SALL4 mutations, Hum. Mol. Genet. 11 (2002) 2979–2987.
[14] R. Al-Baradie, K. Yamada, C. St Hilaire, W.M. Chan, C. Andrews, N. McIntosh, M. Nakano, E.J. Martonyi, W.R. Raymond, S. Okumura, M.M. Okihiro, E.C. Engle, Duane radial ray syndrome (Okihiro syndrome) maps to 20q13 and results from mutations in SALL4, a new member of the SAL family, Am. J. Hum. Genet. 71 (2002) 1195–1199.
[15] J. Kohlhase, M. Heinrich, M. Liebers, L. Frohlich Archangelo, W. Reardon, A. Kispert, Cloning and expression analysis of

SALL4, the murine homologue of the gene mutated in Okihiro syndrome, Cytogenet. Genome Res. 98 (2002) 274–277.
[16] J. Kohlhase, A. Wischermann, H. Reichenbach, U. Froster, W. Engel, Mutations in the SALL1 putative transcription factor gene cause Townes–Brocks syndrome, Nat. Genet. 18 (1998) 81–83.
[17] R. Nishinakamura, Y. Matsumoto, K. Nakao, K. Nakamura, A. Sato, N.G. Copeland, D.J. Gilbert, N.A. Jenkins, S. Scully, D.L. Lacey, M. Katsuki, M. Asashima, T. Yokota, Murine homolog of SALL1 is essential for ureteric bud invasion in kidney development, Development 128 (2001) 3105–3115.
[18] R.P. Kuhnlein, G. Frommer, M. Friedrich, M. Gonzalez-Gaitan, A. Weber, J.F. Wagner-Bernholz, W.J. Gehring, H. Jackle, R. Schuh, Spalt encodes an evolutionarily conserved zinc finger protein of novel structure which provides homeotic gene function in the head and tail region of the *Drosophila* embryo, EMBO J. 13 (1994) 168–179.
[19] S.M. Kiefer, B.W. McDill, J. Yang, M. Rauchman, Murine Sall1 represses transcription by recruiting a histone deacetylase complex, J. Biol. Chem. 277 (2002) 14869–14876.
[20] C. Netzer, L. Rieger, A. Brero, C.D. Zhang, M. Hinzke, J. Kohlhase, S.K. Bohlander, SALL1, the gene mutated in Townes–Brocks syndrome, encodes a transcriptional repressor which interacts with TRF1/PIN2 and localizes to pericentromeric heterochromatin, Hum. Mol. Genet. 10 (2001) 3017–3024.
[21] D. Nellen, R. Burke, G. Struhl, K. Basler, Direct and long-range action of a DPP morphogen gradient, Cell 85 (1996) 357–368.
[22] M. Llimargas, Wingless and its signalling pathway have common and separable functions during tracheal development, Development 127 (2000) 4407–4417.
[23] T. Chihara, S. Hayashi, Control of tracheal tubulogenesis by Wingless signaling, Development 127 (2000) 4433–4442.
[24] H. Niwa, K. Yamamura, J. Miyazaki, Efficient selection for high-expression transfectants with a novel eukaryotic vector, Gene 108 (1991) 193–199.
[25] T. Matsuda, T. Nakamura, K. Nakao, T. Arai, M. Katsuki, T. Heike, T. Yokota, STAT3 activation is sufficient to maintain an undifferentiated state of mouse embryonic stem cells, EMBO J. 18 (1999) 4261–4269.
[26] I. Sakamoto, S. Kishida, A. Fukui, M. Kishida, H. Yamamoto, S. Hino, T. Michiue, S. Takada, M. Asashima, A. Kikuchi, A novel beta-catenin-binding protein inhibits beta-catenin-dependent Tcf activation and axis formation, J. Biol. Chem. 275 (2000) 32871–32878.
[27] Y. Watanabe, T. Tanaka, Y. Uchiyama, T. Takeno, A. Izumi, H. Yamashita, J. Kumakura, H. Iwanari, J. Shu-Ying, M. Naito, D.J. Mangelsdorf, T. Hamakubo, T. Kodama, Establishment of a monoclonal antibody for human LXRalpha: detection of LXRalpha protein expression in human macrophages, Nucl. Recept. 1 (2003) 1.
[28] S. Shibamoto, K. Higano, R. Takada, F. Ito, M. Takeichi, S. Takada, Cytoskeletal reorganization by soluble Wnt-3a protein signalling, Genes Cells 3 (1998) 659–670.
[29] T. Imamura, M. Takase, A. Nishihara, E. Oeda, J. Hanai, M. Kawabata, K. Miyazono, Smad6 inhibits signalling by the TGF-beta superfamily, Nature 389 (1997) 622–626.
[30] W. Ishida, T. Hamamoto, K. Kusanagi, K. Yagi, M. Kawabata, K. Takehara, T.K. Sampath, M. Kato, K. Miyazono, Smad6 is a Smad1/5-induced smad inhibitor. Characterization of bone morphogenetic protein-responsive element in the mouse Smad6 promoter, J. Biol. Chem. 275 (2000) 6075–6079.
[31] K. Nakajima, Y. Yamanaka, K. Nakae, H. Kojima, M. Ichiba, N. Kiuchi, T. Kitaoka, T. Fukada, M. Hibi, T. Hirano, A central role for Stat3 in IL-6-induced regulation of growth and differentiation in M1 leukemia cells, EMBO J. 15 (1996) 3651–3658.
[32] H. de The, M.M. Vivanco-Ruiz, P. Tiollais, H. Stunnenberg, A. Dejean, Identification of a retinoic acid responsive element in the retinoic acid receptor beta gene, Nature 343 (1990) 177–180.
[33] C. Sharpe, N. Lawrence, A. Martinez Arias, Wnt signalling: a theme with nuclear variations, Bioessays 23 (2001) 311–318.
[34] S.M. Kiefer, K.K. Ohlemiller, J. Yang, B.W. McDill, J. Kohlhase, M. Rauchman, Expression of a truncated Sall1 transcriptional repressor is responsible for Townes–Brocks syndrome birth defects, Hum. Mol. Genet. 12 (2003) 2221–2227.
[35] S. Marlin, S. Blanchard, R. Slim, D. Lacombe, F. Denoyelle, J.L. Alessandri, E. Calzolari, V. Drouin-Garraud, F.G. Ferraz, A. Fourmaintraux, N. Philip, J.E. Toublanc, C. Petit, Townes–Brocks syndrome: detection of a SALL1 mutation hot spot and evidence for a position effect in one patient, Hum. Mutat. 14 (1999) 377–386.
[36] D. Sweetman, T. Smith, E.R. Farrell, A. Chantry, A. Munsterberg, The conserved glutamine-rich region of chick csal1 and csal3 mediates protein interactions with other spalt family members. Implications for Townes–Brocks syndrome, J. Biol. Chem. 278 (2003) 6560–6566.
[37] A. Wodarz, R. Nusse, Mechanisms of Wnt signaling in development, Annu. Rev. Cell Dev. Biol. 14 (1998) 59–88.
[38] J. Koipally, E.J. Heller, J.R. Seavitt, K. Georgopoulos, Unconventional potentiation of gene expression by Ikaros, J. Biol. Chem. 277 (2002) 13007–13015.
[39] J. Koipally, J. Kim, B. Jones, A. Jackson, N. Avitahl, S. Winandy, M. Trevisan, A. Nichogiannopoulou, C. Kelley, K. Georgopoulos, Ikaros chromatin remodeling complexes in the control of differentiation of the hemo-lymphoid system, Cold Spring Harb. Symp. Quant. Biol. 64 (1999) 79–86.
[40] K.E. Brown, S.S. Guest, S.T. Smale, K. Hahm, M. Merkenschlager, A.G. Fisher, Association of transcriptionally silent genes with Ikaros complexes at centromeric heterochromatin, Cell 91 (1997) 845–854.
[41] J. Kim, S. Sif, B. Jones, A. Jackson, J. Koipally, E. Heller, S. Winandy, A. Viel, A. Sawyer, T. Ikeda, R. Kingston, K. Georgopoulos, Ikaros DNA-binding proteins direct formation of chromatin remodeling complexes in lymphocytes, Immunity 10 (1999) 345–355.
[42] B.S. Cobb, S. Morales-Alcelay, G. Kleiger, K.E. Brown, A.G. Fisher, S.T. Smale, Targeting of Ikaros to pericentromeric heterochromatin by direct DNA binding, Genes Dev. 14 (2000) 2146–2160.
[43] A. Bauer, S. Chauvet, O. Huber, F. Usseglio, U. Rothbacher, D. Aragnol, R. Kemler, J. Pradel, Pontin52 and reptin52 function as antagonistic regulators of beta-catenin signalling activity, EMBO J. 19 (2000) 6121–6130.
[44] T. Kramps, O. Peter, E. Brunner, D. Nellen, B. Froesch, S. Chatterjee, M. Murone, S. Zullig, K. Basler, Wnt/wingless signaling requires BCL9/legless-mediated recruitment of pygopus to the nuclear beta-catenin–TCF complex, Cell 109 (2002) 47–60.
[45] K. Tago, T. Nakamura, M. Nishita, J. Hyodo, S. Nagai, Y. Murata, S. Adachi, S. Ohwada, Y. Morishita, H. Shibuya, T. Akiyama, Inhibition of Wnt signaling by ICAT, a novel beta-catenin-interacting protein, Genes Dev. 14 (2000) 1741–1749.
[46] K. Takemaru, S. Yamaguchi, Y.S. Lee, Y. Zhang, R.W. Carthew, R.T. Moon, Chibby, a nuclear beta-catenin-associated antagonist of the Wnt/Wingless pathway, Nature 422 (2003) 905–909.
[47] R.A. Cavallo, R.T. Cox, M.M. Moline, J. Roose, G.A. Polevoy, H. Clevers, M. Peifer, A. Bejsovec, *Drosophila* Tcf and Groucho interact to repress Wingless signalling activity, Nature 395 (1998) 604–608.
[48] J. Roose, H. Clevers, TCF transcription factors: molecular switches in carcinogenesis, Biochim. Biophys. Acta 1424 (1999) M23–M37.
[49] N. Barker, A. Hurlstone, H. Musisi, A. Miles, M. Bienz, H. Clevers, The chromatin remodelling factor Brg-1 interacts with beta-catenin to promote target gene activation, EMBO J. 20 (2001) 4935–4943.

[50] R.T. Collins, J.E. Treisman, Osa-containing Brahma chromatin remodeling complexes are required for the repression of wingless target genes, Genes Dev. 14 (2000) 3140–3152.
[51] S. Sachdev, L. Bruhn, H. Sieber, A. Pichler, F. Melchior, R. Grosschedl, PIASy, a nuclear matrix-associated SUMO E3 ligase, represses LEF1 activity by sequestration into nuclear bodies, Genes Dev. 15 (2001) 3088–3103.
[52] H. Yamamoto, M. Ihara, Y. Matsuura, A. Kikuchi, Sumoylation is involved in beta-catenin-dependent activation of Tcf-4, EMBO J. 22 (2003) 2047–2059.
[53] C. Netzer, S.K. Bohlander, L. Rieger, S. Muller, J. Kohlhase, Interaction of the developmental regulator SALL1 with UBE2I and SUMO-1, Biochem. Biophys. Res. Commun. 296 (2002) 870–876.

Available online at www.sciencedirect.com
SCIENCE DIRECT®
Biochemical and Biophysical Research Communications 325 (2004) 961–967
BBRC
www.elsevier.com/locate/ybbrc

Fetal cells in mother rats contribute to the remodeling of liver and kidney after injury

Yu Wang, Hirotsugu Iwatani, Takahito Ito*, Naoko Horimoto, Masaya Yamato, Isao Matsui, Enyu Imai, Masatsugu Hori

Department of Internal Medicine and Therapeutics, Osaka University School of Medicine, Suita, Osaka, Japan

Received 5 October 2004
Available online 5 November 2004

Abstract

Fetal microchimerism indicates a mixture of cells of maternal and fetal origin seen in maternal tissues during and after pregnancy. Controversy exists about whether persistent fetal microchimerism is related with some autoimmune disorders occurring during and after pregnancy. In the current experiment, an animal model in which EGFP positive cells were taken as fetal-origin cells was designed to detect the fetal microchimerism in various maternal organs. Ethanol drinking and gentamicin injection were adopted to induce liver and kidney injury simultaneously. EGFP positive cells were engrafted not only in the maternal circulation and bone marrow, but also in the liver and kidney as hepatocytes and tubular cells, respectively. These results indicate that fetal cells are engrafted to maternal hematopoietic system without apparent injury and they also contribute to the repairing process of maternal liver and kidney.

Keywords: Fetal cells; Microchimerism; Injury; Green fluorescent protein

Microchimerism has been defined as a chimera of small number of cells from different individuals coexisting within tissues. It has been known for many years that there is a bi-directional traffic of maternal cells and fetal cells through the placenta during pregnancy. Fetal microchimerism indicates a mixture of cells of maternal and fetal origin seen in maternal tissues during and after pregnancy. It has been shown that fetal microchimerism persists in some women for more than 27 years after delivery [1,2].

The recognition that fetal cells pass into the maternal circulation and persist for many years has aroused a question of whether or not persistent fetal microchimerism may trigger a maternal immune reaction resulting in what appears to be an autoimmune disorder, because microchimeric fetal cells are semiallogenic to the maternal immune system. Therefore, many studies have focused on the association between fetal cell microchimerism and subsequent development of autoimmune diseases, especially those having features of chronic graft-versus-host disease, such as systemic sclerosis (SSc) [3–7], Sjögren's syndrome (SS) [8,9], primary biliary cirrhosis (PBC) [10], and autoimmune thyroid diseases (AITD) [11,12]. These autoimmune diseases have a predilection for women with childbearing age and often initiate or exacerbate after pregnancy. Although fetal cells are found in the local lesion of these diseases and may react with stimulation by maternal cells when separated and cultured in vitro [13], there is still a controversy about the hypothesis that fetal microchimerism may be the cause of the disease since fetal microchimeric cells are also found in tissues from patients with non-autoimmune diseases such as chronic hepatitis [14] or found in tissues from control subjects with the same frequencies as from patients with autoimmune diseases [4,7]. It is possible that the accumulation of fetal cells in the local lesion may be due to the response to tissue injury and

* Corresponding author. Fax: +81 6 6879 3639.
E-mail address: taka@medone.med.osaka-u.ac.jp (T. Ito).

0006-291X/$ - see front matter © 2004 Elsevier Inc. All rights reserved.
doi:10.1016/j.bbrc.2004.10.105

therefore it may be the consequence rather than the cause of the disease.

Alternatively, there is another possibility that fetal microchimerism might have a beneficial effect on the host rather than a detrimental effect. Srivatsa et al. [11] found fully differentiated thyroid follicle formed by male fetal cells closely attached to and indistinguishable from the rest of the tissue in the thyroid specimen of one female patient with goiter. The possibility that a fetal stem cell could be transplanted and engrafted in the maternal thyroid to form mature thyroid follicles is plausible since several studies have shown that intravenously transplanted hematopoietic stem cells can migrate to sites such as muscle and liver, and be engrafted to the host organs [15–17].

As to the strategy used in the identification of fetal microchimerism in human, male cell markers have been adopted in most studies because of its simplicity. But it is important to note that fetal microchimerism is derived not only from male fetus but also from female fetus. Using male genetic markers might bring deviations to the results of the study.

Therefore, in this study, we have designed an animal model for fetal microchimerism detection where EGFP is set as the marker of fetal-origin cells in the maternal tissues. With this model, we have investigated the fetal cell residence in various maternal tissues.

Materials and methods

Animals. Male transgenic Sprague–Dawley rats carrying the enhanced green fluorescent protein (EGFP) transgene (EGFP rat) and female Sprague–Dawley (SD) rats were purchased from Japan SLC (Hamamatsu, Japan). All rats were maintained at the animal facility of Osaka University School of Medicine. They were allowed to get free access to standard laboratory diet and tap water. The female rats weighing 250–300 g were subjected to the following experiment. All the procedures described here were approved by the Animal Committee of Osaka University School of Medicine.

Animal model of microchimerism and the subsequent induction of liver and renal tubular injury. After mating with a single EGFP male rat and the subsequent delivery of babies, a single SD female rat was kept alone in a cage and burdened with simultaneous liver and renal tubular injury. Ethanol was used to induce chronic liver injury with a method modified from Carmiel-Haggai's report [18]. Gentamicin administration was adopted to evoke gentamicin-induced nephropathy [19,20]. The postpartum rats were supplied with drinking water containing 5% of ethanol, without any free access to automatic tap water. The period of ethanol drinking lasted for at least 30 days. The body weight and the amount of the ethanol-containing water drunk by each female rat were recorded everyday to calculate the ethanol taking dosage. At the same time, these postpartum rats received 60 mg/kg/day of gentamicin (Sigma, St. Louis, MO) by subcutaneous injection for 14 consecutive days after the delivery of babies. The same procedure was repeated after a 2-week interval.

Flow cytometric analysis of mononuclear cells in peripheral blood. The postpartum rats were anesthetized by intra-peritoneal administration of pentobarbital and sacrificed after two cycles of gentamicin injection. Peripheral blood was taken via abdominal aorta and kept in the tube rinsed with heparin in advance. One milliliter of the peripheral blood was set aside for the assay of blood chemistry as described later. Ficoll density separation combined with NH_4Cl-lysis method was adopted to collect mononuclear cells from the peripheral blood. In brief, 2 ml of the peripheral blood was carefully overlaid on 5 ml of Lymphoprep (Axis-shield PoC AS, Oslo, Norway) and centrifuged at 800*g* for 20 min at room temperature. After the centrifuge, a cell fraction, located at the interphase, was collected and washed twice with phosphate-buffered saline (PBS)/2% fetal calf serum (FCS). Then the pellet was resuspended with 0.5 ml PBS/2% FCS and then 7.5 ml of lysis solution [8.26 g/L NH_4Cl /1.0 g/L $KHCO_3$ /0.037 g/L $EDTANa_4{\cdot}HCl$ (pH 7.4)] was added. After gentle mixing, it was incubated at room temperature for 5 min and then centrifuged at 300*g* for 5 min at room temperature. The pellet was washed with PBS/2% FCS twice and resuspended with 0.5 ml PBS/2% FCS. Then the sample was subjected to flow cytometric analysis by FACScan (Becton–Dickinson, San Jose, CA, USA). The mononuclear cells in the peripheral blood of EGFP rats and wild type rats were collected in the same manner and were set as positive and negative controls, respectively.

Flow cytometric analysis of bone marrow cells. The postpartum rats were anesthetized and sacrificed as described above. The bone marrow cells were collected by flushing the tibia and femur with ice-cold heparinized PBS/2% FCS and filtered through 70 μm nylon mesh. After the wash, the cells were resuspended with 2 ml PBS/2% FCS and subjected to flow cytometric analysis.

Measurement of plasma creatinine, BUN, ALT, and AST. Peripheral blood was taken via aorta as described above. Plasma was separated from 1 ml of whole blood by centrifuge at 300*g* for 5 min at 4 °C. Creatinine (Cr), blood urea nitrogen (BUN), aspartate aminotransferase (AST), and alanine aminotransferase (ALT) were measured by using appropriate biochemical methods in a commercial laboratory (SRL, Tokyo, Japan).

Tissue preparation. After blood sample was taken via aorta, organs including kidney and liver were thoroughly perfused through the aorta with ice-cold PBS followed by 4% paraformaldehyde (PFA)/PBS before harvest. The organs were harvested and fixed in 4% PFA/PBS for 6 h at 4 °C in the dark and further in 30% sucrose/PBS overnight at 4 °C in the dark. After that, the tissues were embedded in OCT compound (Sakura Finetechnical, Tokyo, Japan) and kept at −80 °C for cryostat sections.

Immunohistochemistry of fixed frozen samples. Immunohistochemical analysis of frozen sections was performed as described previously [19]. In brief, for albumin staining of the liver, 4-μm fixed frozen sections were incubated with normal goat serum for 30 min first and then with purified IgG fraction of polyclonal rabbit antiserum to rat albumin (Accurate Chemical and Scientific Corporation, Westbury, NY, USA) for 1 h at room temperature. The sections were washed with PBS three times, were incubated with Texas red-conjugated anti-rabbit IgG antibody (Vector Lab, Burlingame, CA, USA) for 30 min at room temperature, and were washed with PBS three times. The nuclei were stained with 4′,6-diamidino-2-phenylindole (DAPI) (Molecular Probes, Eugene, OR, USA) for 3 min at room temperature and then washed with PBS three times. Finally, the sections were mounted with VECTASHIELD Mounting Medium (Vector Lab, Burlingame, CA, USA) and observed under a fluorescence microscope (Nikon Eclipse E600) (Nikon, Tokyo, Japan) with appropriate filters. All images were captured by a digital imaging system connected to a Macintosh computer. For laminin staining of the kidney, the procedure was the same except that rabbit anti-laminin antibody (Monosan, Uden, The Netherlands) was used as a primary antibody.

Results

Existence of EGFP positive cells in maternal peripheral blood

As mentioned in Materials and methods, EGFP positive cells were regarded as the fetal cell origin and were

used as the marker of fetal microchimerism in our experiment. When we analyzed the peripheral mononuclear cells from wild type rats (Figs. 1A–C) and EGFP transgenic rats (Figs. 1D–F), a distinct different pattern of distribution was observed. The majority of the cells from EGFP transgenic rats distributed over 200 on the EGFP intensity scale which formed two sharp peaks while cells from wild type rats distributed in the region less than

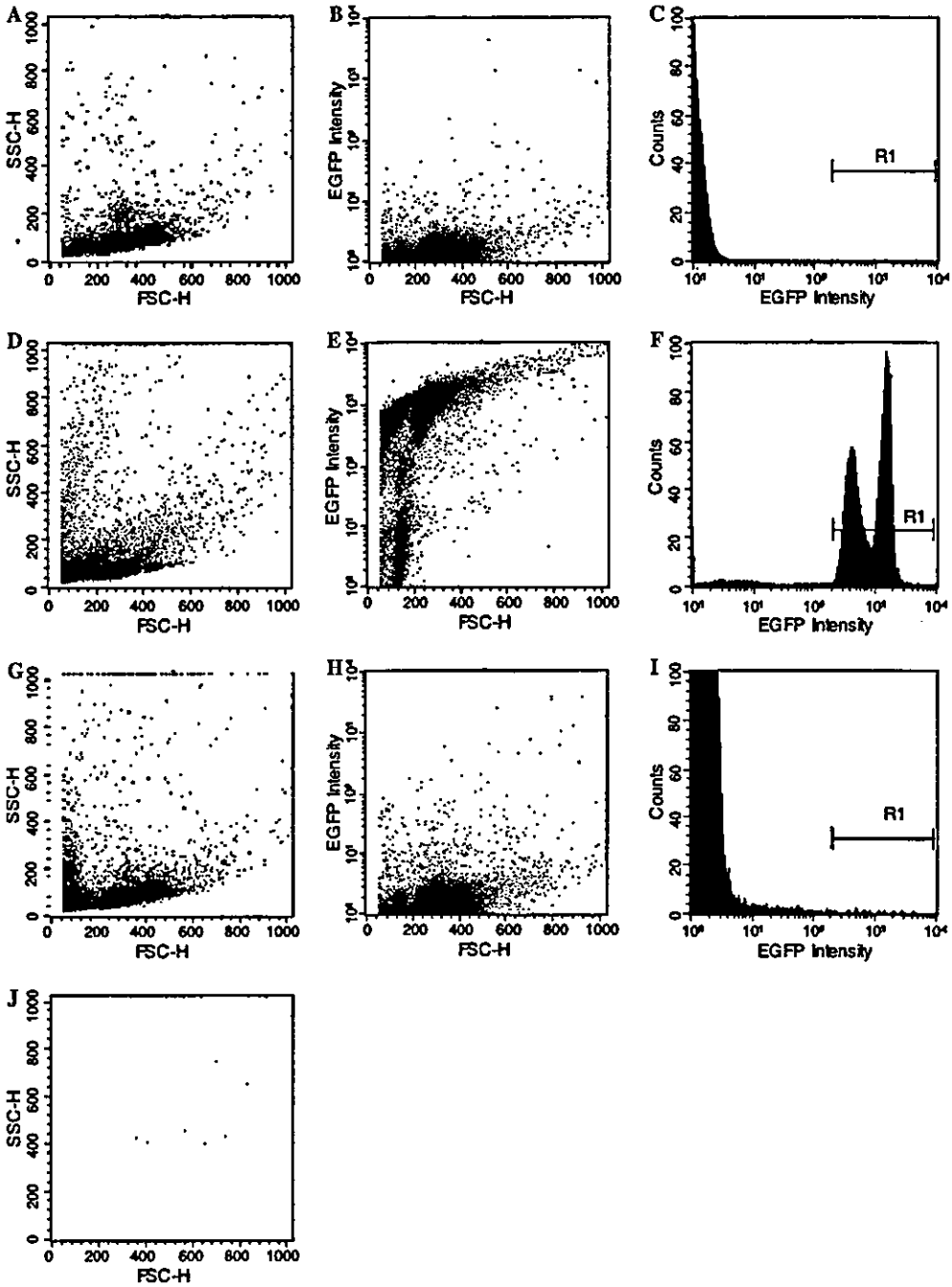

Fig. 1. Flow cytometric analysis of peripheral mononuclear cells. (A–C) Peripheral blood from wild type rats as a negative control. (D–F) Peripheral blood from EGFP transgenic rats as a positive control. (G–J) Peripheral blood from rats treated with gentamicin and ethanol. (A,D,G) The FSC-SSC chart. (B,E,H) The FSC–EGFP chart. (C,F,I) The histogram of EGFP. (J) The FSC–SSC distribution of cells in the R1 region of (I). The distribution pattern indicates that EGFP intensity 200 might be set as the cut-off point to distinguish EGFP positive cells from negative cells. Some cells in our treated rat distributed in the region over 200 on EGFP intensity scale (R1) are EGFP positive cells derived from fetus.

200 on the EGFP intensity scale. This indicates that EGFP intensity 200 might be set as the cut-off point to distinguish EGFP positive cells from negative cells. Based on this cut-off point, we found EGFP positive cells existed in the peripheral mononuclear cells of our treated rats (Figs. 1G–J).

Existence of EGFP positive cells in maternal bone marrow

Bone marrow cells prepared from the treated rats were analyzed in the same manner as that used for peripheral mononuclear cells. EGFP positive cells were also found engrafted in the maternal bone marrow (Figs. 2A–D). This indicates that fetal cells migrated from the maternal circulation and resided in the bone marrow in the absence of apparent injury to the bone marrow.

Engraftment of EGFP positive cells in liver as hepatocytes

Table 1 shows the average amount of daily ethanol consumption during the period of ethanol supply, and the results of blood biochemistry of each rat. The average consumption of ethanol for each rat is over 4 mg/kg/day which is enough to induce liver injury according to Carmiel-Haggai's report [18]. In accordance, the ALT level of all 4 rats was elevated, which supported the existence of liver injury. When the frozen liver specimens were observed under a fluorescence microscope directly,

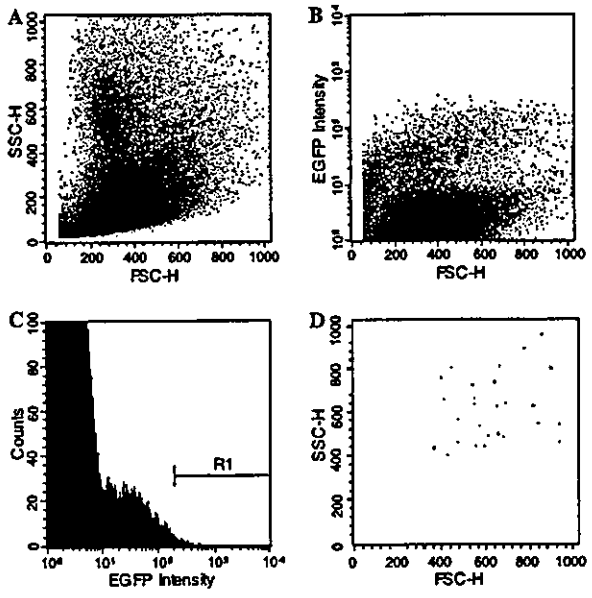

Fig. 2. Flow cytometric analysis of bone marrow cells from rats treated with gentamicin and ethanol. (A) The FSC–SSC chart. (B) The FSC–EGFP chart. (C) The histogram of EGFP. (D) The FSC–SSC chart of cells in the R1 region of (C). There are several cells distributed in the region over 200 on EGFP intensity scale (R1) which are EGFP positive cells originated from fetus.

Table 1
Ethanol consumption and blood chemistry of the rats treated with ethanol and gentamicin

No.	Average consumption of ethanol (g/kg BW/day)	ALT (IU/L)	AST (IU/L)	Cr (mg/dL)	BUN (mg/dL)
1	4.8	36	64	0.43	25.2
2	9.1	36	122	0.31	28.7
3	6.7	63	239	0.91	53.1
4	7.7	42	151	0.21	29.4
	Normal range	24 ± 6.4	68 ± 16.5	0.6 ± 0.11	15.4 ± 2.54

The average consumption of ethanol for each rat is over 4 mg/kg/day which is enough to induce liver injury. The ALT and BUN levels of the 4 rats were all elevated.

EGFP positive cells were found scattered in the liver (Figs. 3A–C). The EGFP positive cells were also positive to albumin (Figs. 3D–F), a marker of hepatocytes. These results indicate that fetal cells contributed to hepatocytes in the maternal injured liver.

Engraftment of EGFP positive cells in kidney as tubular epithelial cells

As shown in Table 1, BUN levels of the 4 rats were all elevated. We have already confirmed that gentamicin nephropathy is a good model for trapping circulating tubular precursor cells in the bone marrow [19]. No EGFP positive cells could be found in the glomeruli because cells expressing EGFP protein were detected within the tubular basement membrane, indicating they were tubular cells. These cells expressed EGFP in a cytoplasmic pattern, which excludes the possibility that we simply observed EGFP endocytosed from the circulation or from the tubular fluid by tubular epithelial cells (Figs. 4A–D).

Discussion

Human fetal cells can be found in the maternal circulation as early as 4–5 weeks of gestation and persist for several decades after delivery [1,2]. The results of the current animal experiment prove the existence of fetal cells in the rat maternal circulation which is in accordance with the previous reports on human, and support the notion that fetal microchimerism is a common phenomenon associated with pregnancy in nature. Furthermore, the finding of fetal cells engrafted in maternal bone marrow, liver, and kidney indicates that fetal cells do not only exist in the peripheral circulation but also migrate from the peripheral circulation and reside in multiple maternal organs.

The majority of the studies on fetal microchimerism have traced male DNA as a marker by PCR or FISH

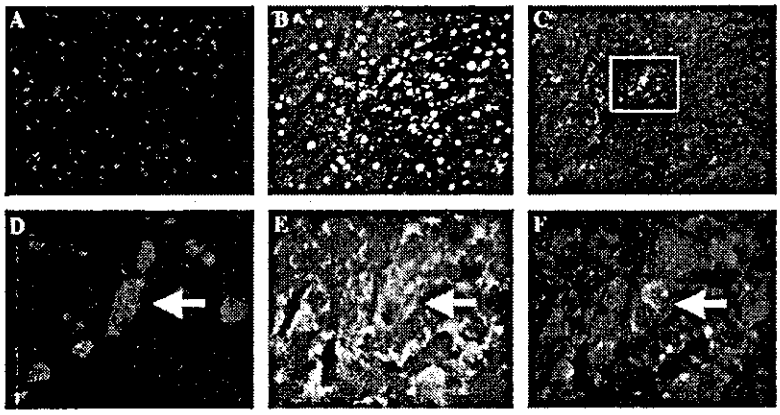

Fig. 3. Chimeric state of liver. (A) Wild type rat as a negative control; (B) EGFP rat as a positive control; (C–F) postpartum rat treated with gentamicin and ethanol; (A,B,D) liver is stained with DAPI. (DAPI, blue) (E) liver is stained with purified IgG fraction of polyclonal rabbit antiserum to rat albumin (Albumin, red) (F) merged image of (D,E) and also an electronically magnified image of rectangle in (C). (Albumin, red; DAPI, blue) arrow in (D) indicates cells which express EGFP in a cytoplasmic pattern. The same cell is pointed by arrow in (E,F). The cell pointed by arrow in (F) is positive to both EGFP and albumin, indicating fetal-derived hepatocyte. Representative images are shown (400×, original magnification).

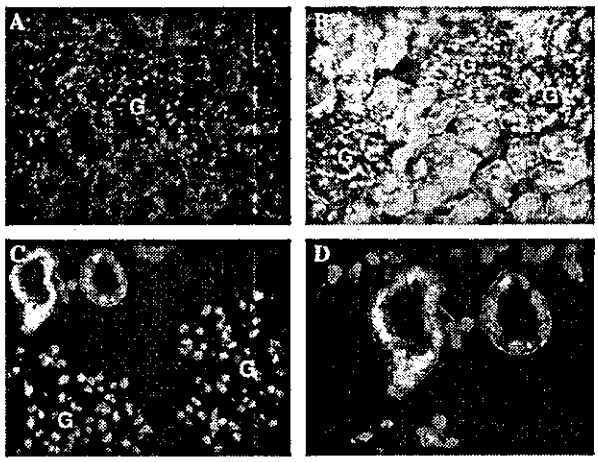

Fig. 4. Chimeric state of kidney. (A) Wild type rat kidney as a negative control; (B) EGFP rat kidney as a positive control; (C,D) kidney from postpartum rat treated with gentamicin and ethanol. A letter G indicates glomeruli. (A–D) Kidney is stained with with anti-laminin antibody and DAPI. EGFP positive cells within the tubular basement membrane in (C) are tubular cells. Laminin, red; DAPI, blue. Representative images are shown [400× for (A,B) 600× for (C) 800× for (D)].

to detect microchimerism in those female hosts who have given birth to or aborted sons. But when targeting male DNA, the particular Y-chromosome sequence can be important. Moreover, fetal cell microchimerism would also exist in mothers who have given birth to daughters but such microchimerism cannot be found out as long as by tracing Y-chromosome. In our experiment, we avoided such problems by mating wild type female rats with EGFP transgenic male rats as employed by Imaizumi's report [21]. EGFP transgenic rats are engineered to express enhanced green fluorescent protein (EGFP) in all cells except for hair and red blood cells, whose expression is driven by cytomegalovirus enhancer and chicken β-actin promoter [22]. Therefore, it is convenient to recognize fetal microchimerism as the EGFP positive cells in the wild type maternal tissues, which can be easily detected by direct observation under a fluorescence microscope regardless of the gender of baby rats.

Chimeric fetal cells are semiallogenic to the maternal immune system. The persistence of semiallogenic fetal cells in maternal solid organs has created an interest in the relationship between these fetal-origin cells and local lesions of some autoimmune diseases with postpartum onset and/or exacerbation. Most evidence comes from the studies on SSc, an autoimmune disease with a characteristic of graft-versus-host disease and with a predilection for women in childbearing age. Nelson et al. [3] found that the frequency of fetal cell microchimerism in circulation was higher in SSc patients than in healthy controls. Artlett et al. [5] reported the same results and also found fetal DNA and cells in skin lesions of SSc women. Ohtsuka et al. [23] reported the existence of significantly higher quantities of fetal DNA in their skin lesions. Similar results have been reported by studies of PBC and AITD. They suggest that fetal cells residing in maternal organs might lead to the local inflammations in such autoimmune diseases. However, Johnson et al. [4] investigated the distribution of fetal cells in various organs of SSc patients and proved that not only the affected organs but also the organs without clinical phenotypes had fetal cells. Johnson et al. [14] also reported the case of fetal microchimerism in liver of chronic hepatitis-C patient which is not an autoimmune disease. Fetal cells were also found in the specimen of non-autoimmune thyroid adenoma [11]. In our animal experiment, fetal cells

were found engrafted not only in maternal bone marrow which was kept intact throughout the experiment, but also in liver and kidney to which injury was induced by chemicals in a non-immunological manner. Thus, the migration and residence of fetal cells in various maternal organs might be a common phenomenon. What seems to be an important factor for the existence of fetal microchimerism in a certain organ could be the cell turnover rate. Bone marrow has a rapid turnover, facilitating engraftment of fetal cells without injury. In kidney or liver, cell turnover is not as rapid as bone marrow [24]. However, in a state where organs are chronically injured with whatever causes, it is likely that fetal microchimerism is established more frequently and detected more easily than in normal physiological state. Given that the accumulation of fetal cells in local lesions of autoimmune diseases might result from changed profiles of inflammatory factors and chemoattractants, inflammatory cells including fetal-origin cells from other organs such as bone marrow can be recruited to the local lesions. Another possibility is in situ proliferation of already engrafted fetal cells in the local lesions because the fetal-origin cells had great power of proliferation under local stimuli in vitro [13]. In our experiments, however, we did not observe EGFP positive cells in non-injured maternal organs (data not shown). Therefore, we assume that recruitment from the circulation to injured organs is the dominant mechanism for establishing chimeric liver and kidney.

Several types of fetal cells have been demonstrated in the maternal circulation during pregnancy, including $CD34^+$ and $CD34^+CD38^+$ hematopoietic progenitor cells [1], nucleated erythroblasts [25], trophoblasts [26], and leucocytes [5]. Persistent fetal hematologic progenitor cells have been detected in maternal peripheral blood as long as 27 years after delivery in human. Fetal leucocytes may play a role in the inflammatory process of the autoimmune diseases. However, fetal progenitor cells might bring different effects on the maternal body. We found that fetal cells join the construction of the maternal organs with the phenotypes which are indistinguishable from their maternal counterparts. Evidence from the research on stem cells of bone marrow has proved that the stem cells reside in the recipient's organs after transplantation and take part in the repair process of the organs in response to injury [15–17]. In the current study, fetal cells resided in the kidney as tubular cells when gentamicin-induced nephropathy was evoked, but no EGFP positive cells were observed in the glomerular region. Gentamicin-induced nephropathy is an animal model of renal tubular injury, and we reported that bone marrow-derived cells are engrafted in renal tubular cells of this animal model [19]. We also reported that intravenously transplanted kidney-derived side population (SP) cells contributed to non-injured liver [19]. These results provide the clue that stem/progenitor cells from fetal microchimerism may engraft liver, kidney, and/or bone marrow, and may take part in the regeneration and reconstruction of renal tubules and/or hepatocytes after injury.

In conclusion, fetal cell microchimerism is a common phenomenon observed in many females after pregnancy. The fetal cells reside not only in the maternal circulation, but also in bone marrow, and in liver and kidney after injury. These fetal cells may take part in the repair process of the maternal organ when injured or during the rest of life even without injury.

Acknowledgments

Yu Wang and Hirotsugu Iwatani equally contributed to this study. This study was supported by grants-in-aid from the Ministry of Education, Science and Culture, Japan (2004), and by grants from Takeda Medical Research Foundation (2004). Yu Wang was supported by JSN-Baxter Scholarship Aid.

References

[1] D.W. Bianchi, G.K. Zickwolf, G.J. Weil, S. Sylvester, M.A. DeMaria, Male fetal progenitor cells persist in maternal blood for as long as 27 years postpartum, Proc. Natl. Acad. Sci. USA 93 (1996) 705–708.

[2] O. Geifman-Holtzman, R.N. Blatman, D.W. Bianchi, Prenatal genetic diagnosis by isolation and analysis of fetal cells circulating in maternal blood, Semin. Perinatol. 18 (1994) 366–375.

[3] J.L. Nelson, D.E. Furst, S. Maloney, T. Gooley, P.C. Evans, A. Smith, M.A. Bean, C. Ober, D.W. Bianchi, Microchimerism and HLA-compatible relationships of pregnancy in scleroderma, Lancet 351 (1998) 559–562.

[4] K.L. Johnson, J.L. Nelson, D.E. Furst, P.A. McSweeney, D.J. Roberts, D.K. Zhen, D.W. Bianchi, Fetal cell microchimerism in tissue from multiple sites in women with systemic sclerosis, Arthritis Rheum. 44 (2001) 1848–1854.

[5] C.M. Artlett, J.B. Smith, S.A. Jimenez, Identification of fetal DNA and cells in skin lesions from women with systemic sclerosis, N. Engl. J. Med. 338 (1998) 1186–1191.

[6] C.M. Artlett, L.A. Cox, R.C. Ramos, T.N. Dennis, R.A. Fortunato, L.K. Hummers, S.A. Jimenez, J.B. Smith, Increased microchimeric CD4+ T lymphocytes in peripheral blood from women with systemic sclerosis, Clin. Immunol. 103 (2002) 303–308.

[7] N.C. Lambert, Y.M. Lo, T.D. Erickson, T.S. Tylee, K.A. Guthrie, D.E. Furst, J.L. Nelson, Male microchimerism in healthy women and women with scleroderma: cells or circulating DNA? A quantitative answer, Blood 100 (2002) 2845–2851.

[8] S. Aractingi, J. Sibilia, V. Meignin, D. Launay, E. Hachulla, C. Le Danff, A. Janin, X. Mariette, Presence of microchimerism in labial salivary glands in systemic sclerosis but not in Sjogren's syndrome, Arthritis Rheum. 46 (2002) 1039–1043.

[9] Y. Endo, I. Negishi, O. Ishikawa, Possible contribution of microchimerism to the pathogenesis of Sjogren's syndrome, Rheumatology (Oxford) 41 (2002) 490–495.

[10] P.A. Fanning, J.R. Jonsson, A.D. Clouston, C. Edwards-Smith, G.A. Balderson, G.A. Macdonald, D.H. Crawford, P. Kerlin, L.W. Powell, E.E. Powell, Detection of male DNA in the liver of

female patients with primary biliary cirrhosis, J. Hepatol. 33 (2000) 690–695.
[11] B. Srivatsa, S. Srivatsa, K.L. Johnson, O. Samura, S.L. Lee, D.W. Bianchi, Microchimerism of presumed fetal origin in thyroid specimens from women: a case-control study, Lancet 358 (2001) 2034–2038.
[12] T. Ando, T.F. Davies, Clinical Review 160: postpartum autoimmune thyroid disease: the potential role of fetal microchimerism, J. Clin. Endocrinol. Metab. 88 (2003) 2671–2965.
[13] S.E. Burastero, S. Galbiati, A. Vassallo, M.G. Sabbadini, M. Bellone, L. Marchionni, M. Smid, E. Ferrero, A. Ferrari, M. Ferrari, L. Cremonesi, Cellular microchimerism as a lifelong physiologic status in parous women: an immunologic basis for its amplification in patients with systemic sclerosis, Arthritis Rheum. 48 (2003) 1109–1116.
[14] K.L. Johnson, O. Samura, J.L. Nelson, M.d.W.M. McDonnell, D.W. Bianchi, Significant fetal cell microchimerism in a non-transfused woman with hepatitis C: evidence of long-term survival and expansion, Hepatology 36 (2002) 1295–1297.
[15] N.D. Theise, S. Badve, R. Saxena, O. Henegariu, S. Sell, J.M. Crawford, D.S. Krause, Derivation of hepatocytes from bone marrow cells in mice after radiation-induced myeloablation, Hepatology 31 (2000) 235–240.
[16] G. Ferrari, G. Cusella-De Angelis, M. Coletta, E. Paolucci, A. Stornaiuolo, G. Cossu, F. Mavilio, Muscle regeneration by bone marrow-derived myogenic progenitors, Science 279 (1998) 1528–1530.
[17] B.E. Petersen, W.C. Bowen, K.D. Patrene, W.M. Mars, A.K. Sullivan, N. Murase, S.S. Boggs, J.S. Greenberger, J.P. Goff, Bone marrow as a potential source of hepatic oval cells, Science 284 (1999) 1168–1170.
[18] M. Carmiel-Haggai, A.I. Cederbaum, N. Nieto, Binge ethanol exposure increases liver injury in obese rats, Gastroenterology 125 (2003) 1818–1833.
[19] H. Iwatani, T. Ito, E. Imai, Y. Matsuzaki, A. Suzuki, M. Yamato, M. Okabe, M. Hori, Hematopoietic and nonhematopoietic potentials of Hoechst (low)/side population cells isolated from adult rat kidney, Kidney Int. 65 (2004) 1604–1614.
[20] D.C. Houghton, M. Hartnett, M. Campbell-Boswell, G. Porter, W. Bennett, A light and electron microscopic analysis of gentamicin nephrotoxicity in rats, Am. J. Pathol. 82 (1976) 589–612.
[21] M. Imaizumi, A. Pritsker, P. Unger, T.F. Davies, Intrathyroidal fetal microchimerism in pregnancy and postpartum, Endocrinology 143 (2002) 247–253.
[22] T. Ito, A. Suzuki, E. Imai, M. Okabe, M. Hori, Bone marrow is a reservoir of repopulating mesangial cells during glomerular remodeling, J. Am. Soc. Nephrol. 12 (2001) 2625–2635.
[23] T. Ohtsuka, Y. Miyamoto, A. Yamakage, S. Yamazaki, Quantitative analysis of microchimerism in systemic sclerosis skin tissue, Arch. Dermatol. Res. 293 (2001) 387–391.
[24] D.W. Kennedy, J.L. Abkowitz, Kinetics of central nervous system microglial and macrophage engraftment: analysis using a transgenic bone marrow transplantation model, Blood 90 (1997) 986–993.
[25] D.W. Bianchi, A.F. Flint, M.F. Pizzimenti, J.H. Knoll, S.A. Latt, Isolation of fetal DNA from nucleated erythrocytes in maternal blood, Proc. Natl. Acad. Sci. USA 87 (1990) 3279–3283.
[26] U.W. Mueller, C.S. Hawes, A.E. Wright, A. Petropoulos, E. DeBoni, F.A. Firgaira, A.A. Morley, D.R. Turner, W.R. Jones, Isolation of fetal trophoblast cells from peripheral blood of pregnant women, Lancet 336 (1990) 197–200.

F. Sato
I. Narita
S. Goto
D. Kondo
N. Saito
J. Ajiro
D. Saga
A. Ogawa
M. Kadomura
F. Akiyama
Y. Kaneko
M. Ueno
M. Sakatsume
F. Gejyo

Transforming growth factor-β1 gene polymorphism modifies the histological and clinical manifestations in Japanese patients with IgA nephropathy

Key words:
gene polymorphism; glomerulonephritis; IgA nephropathy; TGF-β1

Acknowledgments:
This work was supported in part by a Health and Labour Science Research Grants for Research on Specific Diseases from the Ministry of Health, Labour, and Welfare of Japan to Gejyo F. The authors thank Kumiko Furui and Naofumi Imai for excellent technical assistance.

Abstract: Transforming growth factor (TGF)-β1, a multifunctional cytokine, which regulates proliferation and differentiation of a variety of cell types, has the central role in the development and progression of renal injury in both animal models and human. Although it has been suggested that genetic variations in the *TGF-β1* gene are associated with the activity of the gene product, their clinical significance in glomerular disease is unknown. We investigated whether the polymorphisms of *C-509T* and *T869C* in *TGF-β1* account for interindividual variation in manifestations of IgA nephropathy (IgAN) using 626 Japanese subjects including 329 patients with histologically proven IgAN and 297 healthy controls with normal urinalysis. The frequencies of genotypes, alleles, and major haplotypes were similar between the patients and controls. The *C-509T* and *T869C* polymorphisms were in tight linkage disequilibrium, and the major haplotypes were *C-C* and *T-T*, which accounted for more than 95% of the total. In patients with *–509CC* and in those with the *869CC*, urinary protein excretion was higher than in those with other genotypes, whereas no difference in other clinical manifestations was noted. Moreover, patients with *–509CC* and those with *869CC* genotypes presented with a significant higher score of mesangial cell proliferation than in those with other genotypes. These results suggest that TGF-β1 gene polymorphisms are specifically associated with heavy proteinuria and mesangial cell proliferation in Japanese patients with IgAN, although they do not confer susceptibility to this disease.

Authors' affiliation:

F. Sato,
I. Narita,
S. Goto,
D. Kondo,
N. Saito,
J. Ajiro,
D. Saga,
A. Ogawa,
M. Kadomura,
F. Akiyama,
Y. Kaneko,
M. Ueno,
M. Sakatsume,
F. Gejyo

Division of Clinical Nephrology and Rheumatology, Niigata University Graduate School of Medical and Dental Sciences, Niigata, Japan

Correspondence to:
Ichiei Narita
Division of Clinical Nephrology and Rheumatology
Niigata University
Graduate School of Medical and Dental Sciences
1-754, Asahimachi-dori
Niigata 951-8510
Japan
Tel.: +81-25-227-2193
Fax: +81-25-227-0775
e-mail: narital@med.niigata-u.ac.jp

Transforming growth factor-β1 (TGF-β1) is a multifunctional cytokine, which regulates proliferation and differentiation of a wide variety of cell types. *In vitro* studies have suggested that mesangial matrix accumulation, increased fibrosis, and cell proliferation are promoted by TGF-β1 (1, 2) The central role of this cytokine in the development and progression of renal injury has been well documented in both animal models and human diseases (3). Recent evidence indicates the functional roles of TGF-β1 signaling in mediating apoptosis and epithelial-to-mesenchymal transdifferentiation, which have been proposed as putative primary pathomechanisms of progression of renal disease (4). In addition to the central roles of this

Received 9 December 2003, revised 24 February 2004, accepted for publication 24 March 2004

doi: 10.1111/j.1399-0039.2004.00256.x

Tissue Antigens 2004: 64: 35–42

cytokine in the progression of renal disease, TGF-β1 is known to be involved in the class switching to immunoglobulin (Ig)A in B-lymphocytes (5). Because it has been shown that the concentration of TGF-β1 is predominantly under genetic control (6, 7), genetic polymorphisms, which influence the gene transcription or the activity of TGF-β1, may account for the development, as well as the interindividual variation in manifestations of glomerular disease such as primary IgA nephropathy (IgAN).

IgAN, characterized by mesangial proliferative glomerulonephritis with predominant deposits of IgA in the glomerular mesangial area, is the most common form of primary glomerulonephritis, and one of the principal causes of end-stage renal disease (ESRD). Almost 40% of IgAN cases progress to ESRD during the initial 20 years after the onset, whereas the remaining patients have benign renal prognosis (8–10). It has been suggested that, both environmental and genetic factors are involved in the development and progression of this disease (11, 12).

The human gene encoding TGF-β1 (MIM 190180), located on chromosome 19q13, is highly polymorphic. Five polymorphisms in Caucasian populations have been identified: two in the promoter region at position −800 and −509, one at position +72 in a non-translated region, and two in the signal sequence at positions +869 and +915, which change codon 10 (T or C, leucine→proline) and codon 25 (G or C, arginine→proline), respectively (6). For codon 25, the C alelle encoding proline for these polymorphisms is associated with lower TGF-β1 synthesis *in vitro* and *in vivo*. However, there is no gene variation at codon 25 in Japanese (13, 14). In this study, we evaluated two polymorphisms, *C-509T* and *C869T* of *TGF-β1*, because both of them have been reported to be associated with some clinical phenotypes (15–19). Grainger et al. (7) found that the *C-509T* polymorphism was associated with the circulating concentration of TGF-β1, which was significantly lower in subjects with *CC* genotype than with other genotypes in Caucasian women. On the other hand, *CC* genotype of the *T869C* polymorphism was associated with higher TGF-β1 concentration than other genotypes in Japanese (18, 19).

Little is known about the linkage disequilibrium between these two genetic polymorphisms, or their significance in the patients with IgAN. Therefore, in this study, we have investigated the possible association of genetic polymorphism of *C-509T* and *T869C* in *TGF-β1* with the development, as well as the clinical and histopathological manifestations, in Japanese patients with IgAN.

Materials and methods

Study subjects

The ethics committee of our institution approved the protocol for the study, and informed written consent for the genetic studies was obtained from all participants. Japanese patients were eligible for inclusion in the analysis when (1) they had been diagnosed as having IgAN by kidney biopsy at our institute between 1976 and 2002 (2), they had no evidence of systemic diseases such as hepatic glomerulosclerosis, Schönlein-Henoch purpura, and rheumatoid arthritis (3), written informed consent for genetic study was obtained. Among 4587 patients who underwent renal biopsy at our institute between 1976 and 2002, 582 were diagnosed as having IgAN. In total, 329 patients fulfilled the above criteria and were recruited for this study. In all cases, the diagnosis of IgAN was based on a kidney biopsy that revealed the presence of dominant or codominant glomerular mesangial deposits of IgA as assessed by immunofluorescence. The majority of the 253 patients, who did not enter the study, were not included because written informed consent for genetic study was not available.

To provide a control for the local genotype frequency being examined, 297 Japanese volunteers (146 female and 151 male) aged 40 years or older with no history of renal disease and with normal urinalysis were also recruited.

Clinical and histological manifestations

Clinical characteristics of the patients with IgAN at the time of diagnosis including gender, age, body mass index (BMI), urinary protein excretion (g/24 h), serum creatinine (sCr, mg/dl), 24-h creatinine clearance (Ccr, ml/min), serum IgA (mg/dl), and office blood pressures were investigated from their medical records. The time from the first urine abnormality to renal biopsy (month) was also recorded for 245 of the 329 patients, where the first episode of urine abnormality (proteinuria or hematuria) could be clearly defined.

Histopathological findings were classified according to the classification described previously (20). A single pathologist evaluated all specimens by light microscopy in a double blind fashion. Glomerular changes were scored for each glomerulus, and the average score of each patient was calculated. The scores for cellular proliferation and the matrix increase in the mesangium were graded from zero to four as follows: grade 0, no light-microscopic abnormalities; grade 1, segmental mild proliferation of mesangial components; grade 2, segmental moderate or global mild proliferation of mesangial components; grade 3, segmental sclerosis or global moderate proliferation of mesangial components; and grade 4, global sclerosis or global marked proliferation of mesangial components.

Other glomerular changes including endocapillary proliferation, duplication of glomerular basement membrane (GBM), crescent formation, and adhesion of tufts to Bowman's capsule as well as tubulointerstitial lesions were graded from zero to four according to their